ZOOPLANKTON VARIABILITY IN THE CALIFORNIA CURRENT, 1951–1982

COLLIN S. ROESLER AND DUDLEY B. CHELTON
College of Oceanography
Oregon State University
Corvallis, Oregon 97331

ABSTRACT

Seasonal and nonseasonal variations in zooplankton biomass in the California Current system are examined from CalCOFI measurements over the period 1951–82. Seasonal signals indicate that total biomass and degree of seasonality are greater in the northern regions, and springtime blooming is initiated in the northern nearshore regions up to two months earlier than in the southern and far offshore regions. Semiannual variability in both zooplankton biomass and geostrophic flow is a common feature throughout the CalCOFI sampling region, suggesting a relationship between zooplankton variability and advection of nutrients and zooplankton biomass. Throughout most of the study area maxima/minima in seasonal zooplankton biomass lag maxima/minima in seasonal alongshore geostrophic flow by one month or less. This indicates that seasonal advection of biomass into the CalCOFI sampling area dominates the observed seasonal fluctuations in local zooplankton abundances.

Nonseasonal zooplankton biomass variability is examined using empirical orthogonal function (EOF) analysis. The principal EOF pattern of $\log_e$ transformed zooplankton volumes is dominated by low-frequency (interannual) variability that is clearly coupled to variations in the transport of the California Current. The timing of zooplankton biomass variations relative to variations in southward advection suggests that nonseasonal zooplankton biomass variations are controlled by two processes: (1) the response of local zooplankton populations to advection of zooplankton biomass—the dominant process in the north—and (2) the response of local zooplankton populations to nutrient advection or the development of more favorable environmental conditions caused by changes in advection—processes that become increasingly dominant from north to south. Examination of the biogeographic boundaries of 15 of the dominant zooplankton species in the survey area during periods of strong current variations also indicate that these mechanisms control the low-frequency zooplankton variability.

The variability of non-$\log_e$ transformed zooplankton biomass is dominated by episodic pulses with time scales less than three months. The spatial pattern associated with the first EOF of untransformed zooplankton suggests a northern source of variability centered offshore in the core of the California Current. The ephemeral nature of the signal suggests a response to nutrients and phytoplankton injected into the core of the California Current by one or more coastal jets or filaments, resulting in an isolated population that dies out relatively quickly (two to three months) for lack of continued food supply in offshore regions.

[Manuscript received March 11, 1987.]

RESUMEN

Las variaciones estacionales y no-estacionales en la biomasa de zooplancton colectada por CalCOFI son examinadas para el período 1951–82. Los marcadores estacionales indican que la biomasa total y el grado de estacionalidad son mayores en las regiones del norte, y que el aumento en la primavera comienza dos meses o menos antes en las regiones costeras del norte que en aquellas al sur o mar adentro. La variabilidad semianual tanto en la biomasa zooplanctónica como en el flujo geostrófico es una característica común a toda la zona muestreada por CalCOFI, sugiriendo una relación entre la variabilidad del zooplancton y la advección de nutrientes y biomasa zooplanctónica. Los máximos y mínimos estacionales de la biomasa zooplanctónica están atrasados en un mes o menos con respecto a los máximos y mínimos estacionales del flujo geostrófico a lo largo de la costa. Esto indica que una advección estacional de biomasa hacia el área de muestreo de CalCOFI domina las fluctuaciones observadas en las abundancias locales de zooplancton.

La variabilidad no-estacional en la biomasa zooplanctónica es examinada por medio del análisis de una función empírico-ortogonal (FEO). El patrón principal del FEO de los volumenes de zooplancton transformados logarítmicamente está dominado por una variabilidad de baja-frecuencia (interanual) la cual está claramente relacionada con variaciones en el transporte de la Corriente de California. La relación temporal de las variaciones de la biomasa zooplanctónica en relación a las varia-

ciones en el proceso de advección con dirección sur sugiere que las variaciones no-estacionales de la biomasa zooplanctónica son controladas por dos procesos: (1) la respuesta de las poblaciones locales de zooplancton a la advección de la biomasa de zooplancton—el proceso dominante en la zona norte—y (2) la respuesta de las poblaciones locales de zooplancton a la advección de nutrientes o el desarrollo de condiciones ambientales más favorables causado por cambios en la advección—aquellos procesos que cobran mayor importancia de norte a sur. El examen de los límites biogeográficos de quince de las especies de zooplancton dominantes en el área investigada durante aquellos períodos de grandes variaciones en las corrientes corroboran el control de la variabilidad de baja frecuencia del zooplancton por estos mecanismos.

La variabilidad de la biomasa de zooplancton no transformada logarítmicamente está dominada por pulsaciones episódicas con escalas de tiempo inferiores a tres meses. Los patrones espaciales asociados con el primer FEO del zooplancton sin transformar sugiere una fuente de variabilidad ubicada al norte, mar adentro, en el centro de la Corriente de California. La naturaleza efímera de esta señal sugiere una respuesta a los nutrientes y fitoplancton inyectados al centro de la Corriente de California por uno o más chorros o filamentos costeros, la cual produce una población aislada que perece en forma relativamente rápida (dos o tres meses) debido a la falta de una fuente de alimentación continua en las regiones mar adentro.

INTRODUCTION

The waters off the west coast of North America have long been observed to be some of the more biologically productive in the world ocean (Reid 1962; Wooster and Reid 1963). The physical processes responsible for the complexity of the eastern boundary current structure and mixture of regional water masses greatly influence the magnitude of biological production in the region. Of utmost biological importance is the source of nutrients to support the high production. This study reviews the processes responsible for the distribution of nutrients in the California Current system (advection and upwelling) and examines how variations in the supply of nutrients affect local biological production. In particular, the seasonal and nonseasonal signals observed in zooplankton displacement volumes from the CalCOFI 32-year time series (1951–82) are analyzed to investigate physical and biological controls.

The upper-ocean water-mass characteristics of the California Current are largely controlled by the source waters in the Alaskan Subarctic Gyre (Hickey 1979). The subarctic water mass is characterized by cold temperature, low salinity, high nutrients, and large standing stocks of zooplankton (Reid 1962). Charting the southern extent of subarctic water influence in the California Current gives some indication of the degree of equatorward transport of nutrient-rich northern waters into the subtropical water mass (characterized by higher temperatures and salinities and smaller standing stocks of zooplankton). An individual water mass is identifiable by some conservative and distinct property. Bernal (1979, 1981) and Bernal and McGowan (1981) have identified characteristically low salinity values (33.4‰) with the subarctic water mass, to distinguish it from the subsurface equatorial/subarctic mixture that is upwelled with salinities greater than 33.8‰ (also characterized by low temperatures and high nutrients).

Salinity maps constructed by the NORPAC Committee (1960) for July through September (the period of strong equatorward transport in the California Current) indicate that the 33.4‰ isohaline can be traced from the surface to depths greater than 200 m. At 10 m below the surface the isohaline extends southward to San Diego in a tongue approximately 1,000 km wide. At 100-m depth the subarctic mass, still a tongue, narrows and extends as far south as the tip of Baja California. At 200 m—the approximate depth of the core of the poleward-flowing undercurrent (Hickey 1979)—the 33.4‰ isohaline is nonexistent in the California Current region. Thus, the zone of subarctic water-mass influence is a large-scale tongue extending from the subarctic gyre thousands of kilometers equatorward (to 25°N), and from the surface to depths shallower than 200 m. The low-salinity subarctic water mass is associated with high nutrients (Reid 1962); clearly, variations in equatorward transport in the California Current could have considerable impact on the biology of the region.

Previous studies of zooplankton variability in the California Current system have found significant correlations between zooplankton biomass and advection (Bernal 1979, 1981; Bernal and McGowan 1981; Chelton et al. 1982; Hemingway 1979). These earlier studies have suggested that zooplankton biomass responds locally to changes in primary productivity caused by variations in the supply of nutrients by advection from the north. However, in all of the studies, the coarseness of the temporal or spatial scales meant that only associative relations could be resolved.

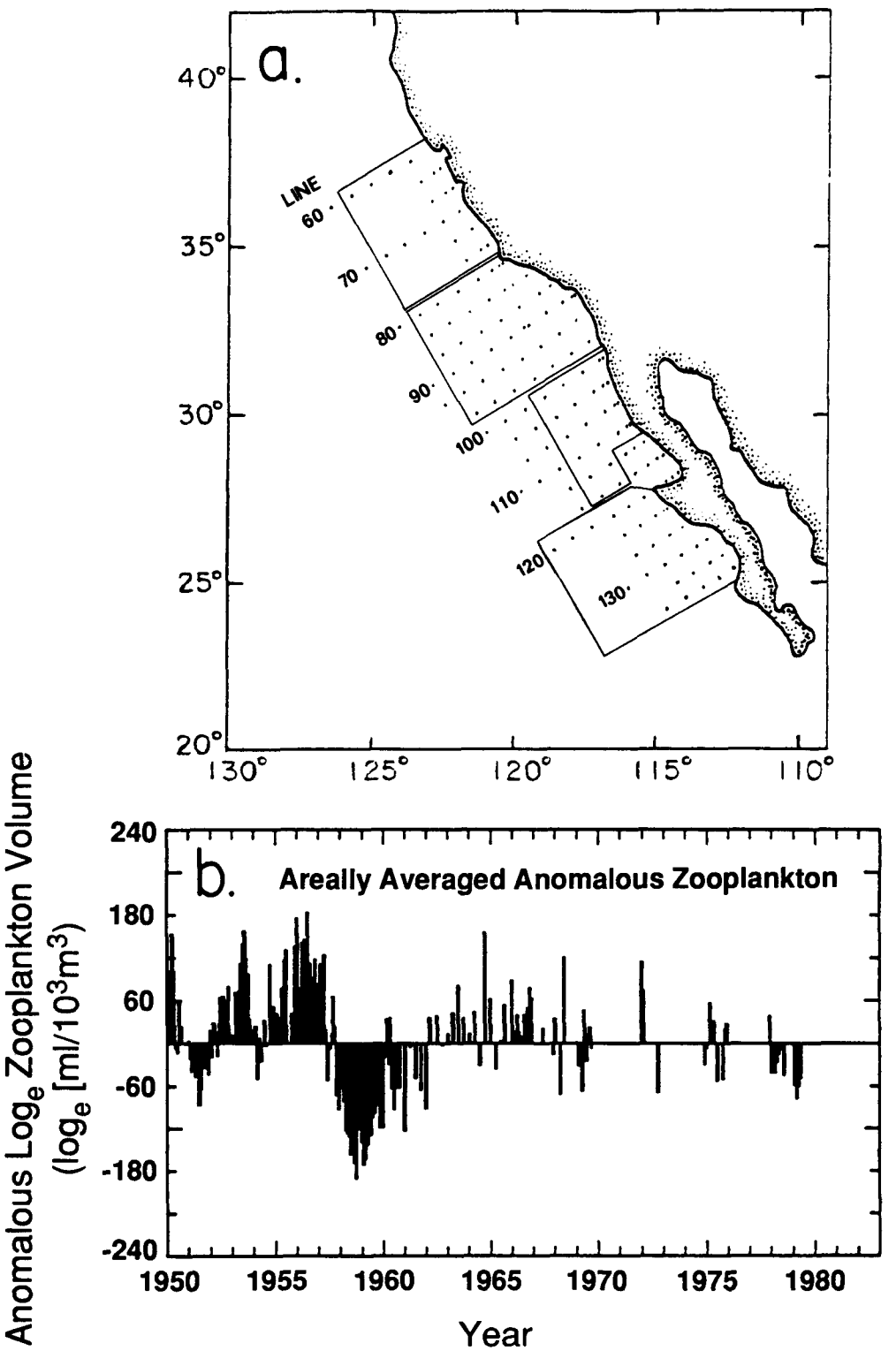

Figure 1. *a*, CalCOFI grid pattern (indicated by dots) and the four regions of average zooplankton volumes used in the study of Chelton et al. (1982). Cardinal lines are denoted by their numbers (60–130). *b*, Areally averaged time series of seasonally corrected (anomalous) zooplankton volumes for the four regions outlined in *a* (also from Chelton et al. 1982).

From a detailed analysis of CalCOFI data for the period 1955–59, Colebrook (1977) showed that large-scale variability in zooplankton was coherent between the taxa, suggesting that fluctuations must result from some physical process rather than from a purely biological interaction. He also concluded that the source of the variability must originate in the north or must affect northern populations to a greater extent. It is noteworthy that Colebrook did not remove the seasonal cycle in his analysis, so his

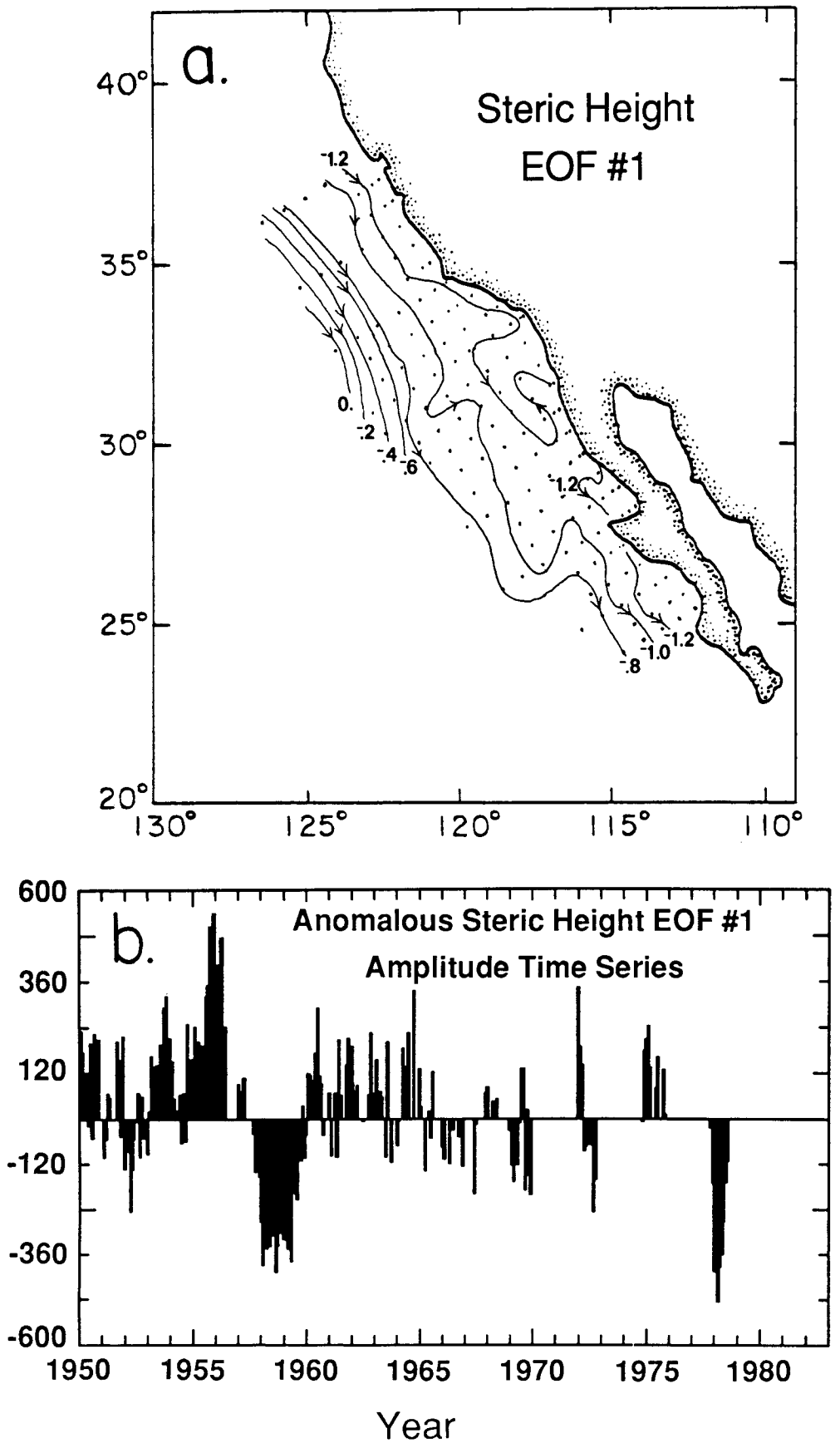

Figure 2. *a*, Spatial pattern of the dominant-mode EOF of anomalous 0/500 db steric height computed from stations (denoted by dots) occupied more than 34 times in the record (1950–78). *b*, The amplitude time series of the dominant EOF mode of steric height. This mode is an index of southward transport in the California Current (from Chelton et al. 1982). Arrows in *a* indicate the direction of the flow when the time series is positive. Weakened or reversed flow occurs when the time series is negative.

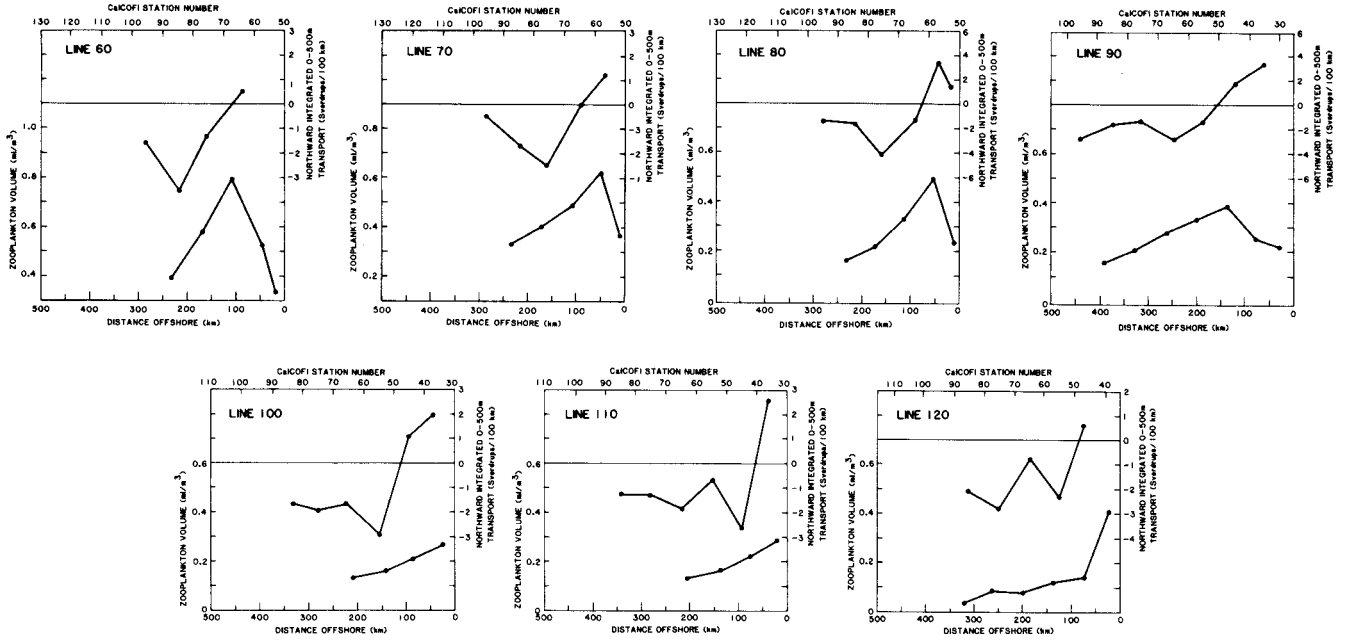

Figure 3. The seasonal values (computed from long-term averages) of the April-through-August averaged zooplankton volumes (ml/10^3m^3), *lower panel*, and the July alongshore integrated transport (in Sverdrups/100 km), *upper panel*, along the CalCOFI cardinal lines. Crossing of the zero axis indicates horizontal shear in the flow (from Chelton 1982a).

results may be strongly influenced by normal seasonal fluctuations in zooplankton biomass.

Chelton et al. (1982) examined large-scale variability in the seasonally corrected total zooplankton displacement volume time series pooled into four areal averages (Figure 1a). Within each of the four areas they found a low-frequency signal of variability with autocorrelation time scales ranging from 14 months in the northern region to 24 months in the southern region (these time scales correspond to periods of about 2.5 to 4.0 years). In order to extract the very large-scale variability, the four regional time series were averaged (Figure 1b). This large-scale average zooplankton time series was found to be significantly correlated with an index of large-scale, nonseasonal advection in the California Current. This index of advection (Figure 2b) was the amplitude time series of the dominant empirical orthogonal function (EOF) of dynamic height at the surface relative to 500 db. Because of the coarse areal averaging of the zooplankton volumes, the detailed spatial structure of the variability was never resolved for comparison with the spatial structure of the advection index (Figure 2a). Furthermore, the detailed mechanisms by which the advective processes affect zooplankton were not defined.

A second study of the CalCOFI zooplankton data by Chelton (1982a) suggested a possible relationship between seasonal geostrophic flow, wind stress curl, and zooplankton abundance. Figure 3 shows the cross-shore signals of averaged zooplankton for April through August (lower panel) and the averaged, vertically integrated, alongshore transport for July (upper panel) in the California Current. Note the horizontal shear in alongshore transport as indicated by poleward transport nearshore and equatorward transport offshore. Between San Francisco and San Diego (CalCOFI lines 60–90), peak zooplankton biomass is found in the region of strongest horizontal shear (the zero crossing of the alongshore transport curve; also found by Bernal 1981). Chelton (1982a) hypothesized that this offshore maximum zooplankton biomass may be related to an offshore maximum wind stress curl causing surface-water divergence and upwelling of deeper waters. This Ekman pumping process leads to an upward tilting of the isopycnals and the nutricline, which brings nutrient-rich deep waters into the euphotic zone. Although spatial correlation between the summer seasonal signals of zooplankton biomass and horizontal shear in the flow is evident from Figure 3, no statistical analyses have yet been performed to establish temporal correlations between the signals.

There are a number of unanswered questions from these earlier studies of CalCOFI zooplankton data: What is the detailed spatial structure of nonseasonal zooplankton variability? Is the low-frequency signal in zooplankton variability identified

by Chelton et al. (1982) a response to variability in advection of nutrients and subsequent local growth, a local response to changing temperature and salinity conditions caused by variability in the advection of northern waters, or the result of actual transport of northern stocks of zooplankton biomass? Finally, is there temporal coherence between the offshore zooplankton maximum and horizontal shear in the flow? These questions are investigated in this study using time series of total zooplankton volume on a sampling grid of greater spatial density than was available for the earlier studies.

DATA DESCRIPTION AND METHODS

One of the important features of the CalCOFI zooplankton sampling strategy has been the maintenance of a fixed sampling grid throughout the measurement program, which began in 1951. Surveys are conducted along parallel lines, approximately normal to the coast and separated by 74 km. The lines separated by 222 km, called cardinal lines, are sampled more frequently (Figure 1a). The first ten years of data were collected at monthly intervals with few interruptions. In 1961, the nearly continuous monthly sampling was replaced with quarterly sampling (every three months). This sampling strategy continued until 1969, when CalCOFI switched to monthly samples every third year. As a consequence of this temporal sampling pattern, any time series analysis of CalCOFI data will be largely dominated by the patterns that occurred in the first ten years of uninterrupted collection. A further description of the sampling strategy and its limitations can be found in Chelton (1981) and Chelton et al. (1982).

Zooplankton displacement volumes are measured by oblique net tows from depths of 140 m to the surface. The 5-m-long nets have a 1-m-diameter opening and are made of 500-μm mesh. With a ship speed of two knots, the nets are retrieved at 20 m per second, filtering a total volume of approximately 500 m^3 of water. The zooplankton volumes used in this study consist of the total amount of zooplankton biomass retrieved from the nets minus all zooplankton exceeding 5 cc and all adult and juvenile fish. For a more complete description of the methods of collection and techniques in processing the zooplankton displacement volumes see Smith (1971) and Kramer et al. (1972).

Zooplankton displacement volumes measured in the CalCOFI region during the period of January 1951 through March 1982 were kindly provided by Paul E. Smith at the National Marine Fisheries

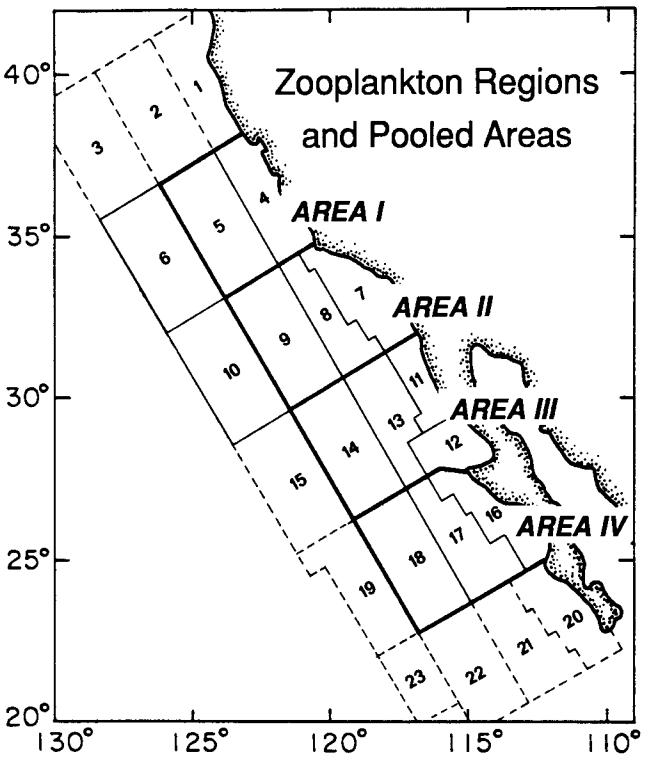

Figure 4. Location of the 23 geographical regions for which spatially averaged CalCOFI zooplankton time series are available (provided by Paul E. Smith). The 14 regions outlined by the solid borders form the basis for the analysis presented in this study; the remaining 9 regions (dashed lines) were deemed to have too few observations over the 32-year record to be useful in this study. The four large-scale areas outlined by heavy borders and labelled as areas I, II, III, and IV are used in the temporal analyses of nonseasonal zooplankton and large-scale advection. These areas are essentially the same as those used previously by Chelton et al. (1982); see Figure 1.

Service in La Jolla, California. Monthly averages were provided for the 23 spatial regions (Figure 4) originally proposed by Smith and used by Colebrook (1977) to filter out short-term fluctuations (such as vertical migration) and small-scale spatial variability (patchiness). Fourteen of the 23 regions were deemed to have adequate temporal coverage over the 32-year record to be useful in this study. Although 9 regions were omitted from the analyses presented here, the remaining 14 regions more than triple the spatial resolution of previous studies of zooplankton variability in the California Current, with little sacrifice of the temporal resolution.

It is customary in analysis of biological data to apply a $\log_e$ transformation to the observed values before analysis. One of the motivations for this transformation is to normalize frequency distributions (Chatfield 1975) in order to place confidence limits on statistical analyses (see Appendix 1). In addition, biological data bases involve, in most cases, exponential growth and decay in the time series. Log_e transforms of data values reduce exponentials to linear representations. Another mo-

tivation, and the most biasing, is to de-emphasize spurious or noisy data points; the $\log_e$ transformation reduces the relative amplitude of extreme values. Thus, applying the $\log_e$ transformation is effectively equivalent to presupposing that peak values are not significant. This is misleading in that a true signal of spiky values will be obscured under the transformation and lost in the analysis (see Appendix 1 for further explanation and examples). In order to determine the consequences of taking the $\log_e$ transformation of the displacement volumes, all analyses presented here were performed on both raw and $\log_e$ transformed time series of total zooplankton volumes for the 14 regions.

The CalCOFI hydrographic stations occupied more than 34 times between 1950 and 1978 are shown in Figure 2a. Temperature and salinity profiles at these stations were used to compute density and specific volume (the reciprocal of density) profiles at each station. The difference between the observed specific volume at each sampled depth and the specific volume of a standard seawater sample (with temperature of 0°C, salinity of $35^0/_{00}$) at the same depth is the specific volume anomaly. Integration of this quantity over the pressure range 0–500 db results in values of steric height of the sea surface relative to the 500-db reference level.

Gradients in steric height from station to station are proportional to the magnitudes of geostrophic flow at the surface relative to the flow at the 500-db level (assumed small). Since alongshore flow in the CalCOFI study area is predominantly equatorward (Hickey 1979; Chelton 1984), the alongshore geostrophic flow in all but the three northernmost zooplankton regions was computed along the northernmost cardinal line located in each region; in regions 4, 5, and 6, line 70 was used rather than line 60 because sampling along line 60 was much less frequent over the 32-year measurement program. The regional alongshore component of geostrophic flow was computed from steric height gradients using the equation:

$$v = \frac{-g}{f}\frac{\Delta h}{\Delta x}$$

where v is the geostrophic velocity, Δx is the distance separating the two stations, f is the Coriolis parameter ($2\Omega\sin\phi$, ϕ is the mean latitude), g is the gravitational acceleration, and Δh is the steric height difference relative to 500 db (offshore minus inshore station).

It should be noted that small errors in steric height at one station are amplified in the geostrophic flow computation to a much greater degree when the stations are close together. For example, in a region of 10 cm/sec flow, a 0.5-cm error in steric height at one station results in a computed flow of 10.5 cm/sec if the stations are separated by 100 km; for stations separated by 10 km, the computed flow is 15.0 cm/sec, an order of magnitude increase in error. Sampling error manifestations in geostrophic flow can be effectively reduced by careful selection of station pairs. In this study, station separations of 74 km were used for the narrow, nearshore zooplankton regions, and 158-km spacings were used for the wider, offshore stations.

The time series of zooplankton volumes and steric height are dominated by seasonal variability. The method used here to estimate the seasonal cycles of zooplankton and steric height is the same as that used previously for the CalCOFI steric height data by Chelton (1981, 1982a) and Chelton et al. (1982). The seasonal cycles in each of the 14 regions shown in Figure 4 were defined by harmonic analysis in which the 12 monthly seasonal values are estimated by multivariate regression of the full 32-year time series on an annual and semiannual cycle. With gappy time series such as the CalCOFI zooplankton and steric height data, a small number of spurious points can significantly alter the harmonic seasonal cycle. Chelton (1984, appendix) discusses this problem in detail. In essence, the fewer the number of samples used in the regression, the more unstable the seasonal cycle. The regions in Figure 4 excluded from analysis in this study were rejected on the basis of too few samples to reliably resolve the seasonal cycles. It should be noted, however, that the reliability of the seasonal cycles for the regions retained for analysis may still be questionable in some cases.

Although seasonal fluctuations are important to a large range of applications, they cannot be analyzed statistically to infer cause-and-effect relationships with any degree of reliability. This is discussed in detail in Chelton (1982b). Briefly, the problem is that seasonal cycles consist of only 12 non-independent data values, so that statistical relationships between two seasonal cycles are based upon a very limited number of degrees of freedom. When the annual and semiannual cycles are used for the harmonic analysis, the seasonal cycles contain only four degrees of freedom, and thus anything less than nearly perfect correlation is not statistically significant. It is therefore essential that seasonal cycles be removed from the raw data before statistical analysis. Removal of the zooplankton seasonal cycle from the respective regional time series results in 14 time series of anomalous

zooplankton volumes. Defining $\hat{z}_n(t)$ to be the $\log_e$ transformed raw zooplankton volume in region n for the month t, and $s_n(t)$ to be the seasonal $\log_e$ transformed zooplankton volume in region n for the corresponding calendar month, the nonseasonal or anomalous $\log_e$ zooplankton volume is given by:

$$z_n(t) = \hat{z}_n(t) - s_n(t).$$

Anomalies of non-$\log_e$ transformed zooplankton volumes are defined similarly. The seasonal cycles of zooplankton and geostrophic flow are presented and discussed in the next section. Statistical analyses of anomalous zooplankton and steric height variability are presented in subsequent sections of this paper.

SEASONAL VARIABILITY

Contour maps of the seasonal cycles of zooplankton displacement volumes are shown in Figure 5. The expected north-south gradient in zooplankton biomass is apparent throughout the year, with northern values being one to six times larger than southern values. Superimposed on the persistent, north-south gradient is a strong cross-shore gradient that begins to intensify in March, reaches a maximum in May, and decreases through September. Highest values of zooplankton biomass are found near shore. The cross-shore gradient is always strongest in the northern regions. The most southerly regions (at 25°N) and the offshore regions (500 km offshore) show comparatively little seasonality. This is perhaps due to the low mean biomass in these areas, which limits the potential range of seasonal fluctuations compared to potentially large fluctuations in areas of higher mean biomass.

The seasonal cycle time series of zooplankton for each of the 14 regions are shown in Figure 6. The 32-year overall mean value of zooplankton biomass for each region is included in the figure to illustrate the alongshore and cross-shore gradients in the annual average zooplankton biomass. The range of seasonal zooplankton variability is much larger in the north. Not surprisingly, the maximum zooplankton biomass generally occurs in the springtime in response to phytoplankton blooms after the onset of increasing daylength and a high supply of nutrients from upwelling and alongshore advection. A noteworthy feature is the presence of a secondary fall or winter maximum in many of the regions. There is no evidence for such semiannual variability in the wind field in this region, so some other mechanism must be responsible for the observed semiannual zooplankton variations.

It is apparent from Figure 6 that spring blooms occur in the northern regions one to two months earlier than in the southern and offshore regions, notably out of phase with the seasonal progression of upwelling winds from south to north (Nelson 1977; Hickey 1979). These results conflict with the conclusions of Loeb et al. (1983), who found only spring blooms of zooplankton occurring in the southern regions first, synchronous with seasonal coastal upwelling. However, their results were based upon only one year of data (1975) and are apparently not representative of the long-term average pattern. Their conclusion that spring blooms of zooplankton are controlled by coastal upwelling is not true for the 32-year average seasonal pattern, observed on the large spatial scales resolvable by the 14 areal averages analyzed here (Figure 4). Factor analysis of a single year of samples by Hemingway (1979) also supports this claim. He found that standing stocks of zooplankton are not associated with coastal upwelling factors or with the standing stocks of phytoplankton confined to the coastal upwelling band.

The conclusion that seasonal variability of zooplankton is not predominantly controlled by upwelling is rather surprising. A number of previous studies have presented evidence that maximum upwelling zones are coherent with maximum zooplankton volumes. Traganza et al. (1981) found microplanktonic blooms (comprising bacteria, algae, and microzooplankton) at the frontal zones of upwelling regions and upwelling plumes. In addition, Smith and Eppley (1982) found zooplankton associated with peak primary productivity at the coast during upwelling times. Smith et al. (1986) found blooms of *Calanus pacificus* occurring in the nutrient- and phytoplankton-rich upwelling frontal zones off Point Conception. They hypothesized that strong upwelling advects postdiapausal individuals into the surface waters of the frontal zones, and they suggest that offshore movement of these frontal zones may contribute to the offshore zooplankton biomass peak observed by Bernal (1981) and Chelton (1982a).

The apparent discrepancies between this study and these earlier studies is most likely due to the different spatial scales addressed in the respective data sets. The boundary of the frontal zones associated with coastal upwelling is determined by the spatial scale of deformation of the density field of the coastal waters caused by wind stress (Pedlosky 1979). This scale, termed the Rossby radius of de-

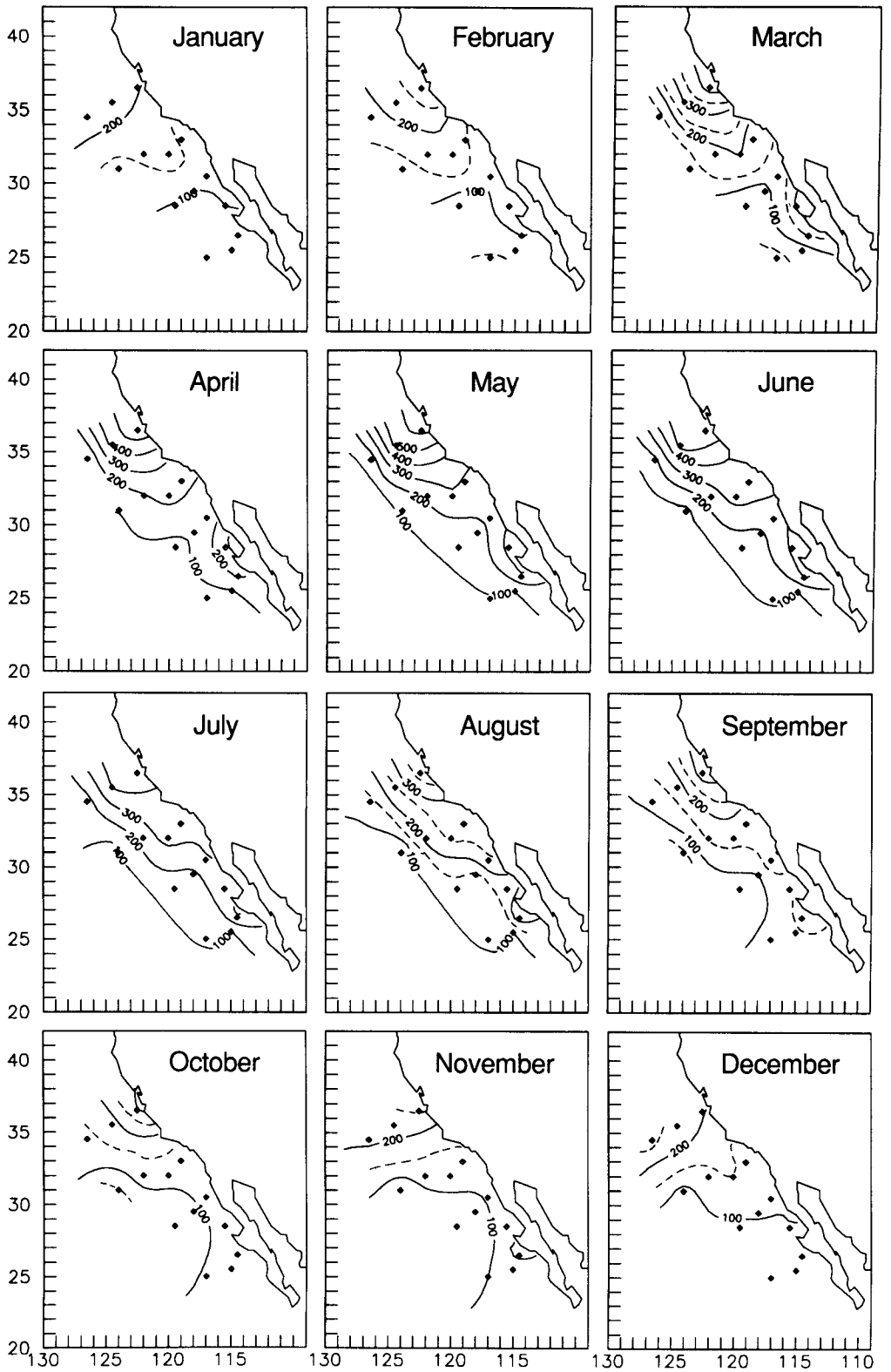

Figure 5. Contour maps of monthly norms of zooplankton displacement volumes in the study area computed from harmonic analysis of the 32-year record. Contour intervals are 100 ml/10^{3}m^3. In months of low biomass, median-valued contours (*dashed lines*) are included for detail of biomass distribution.

formation, is much smaller than the spatial scale of the wind stress and is proportional to water depth. The effective horizontal scale of coastal upwelling is 20 km (Barber and Smith 1981), and the associated offshore transport of upwelled waters is usually within 50 km of the California Coast (Allen 1973; Barber and Smith 1981; Yoshida 1967). Therefore, vertically advected zooplankton in the

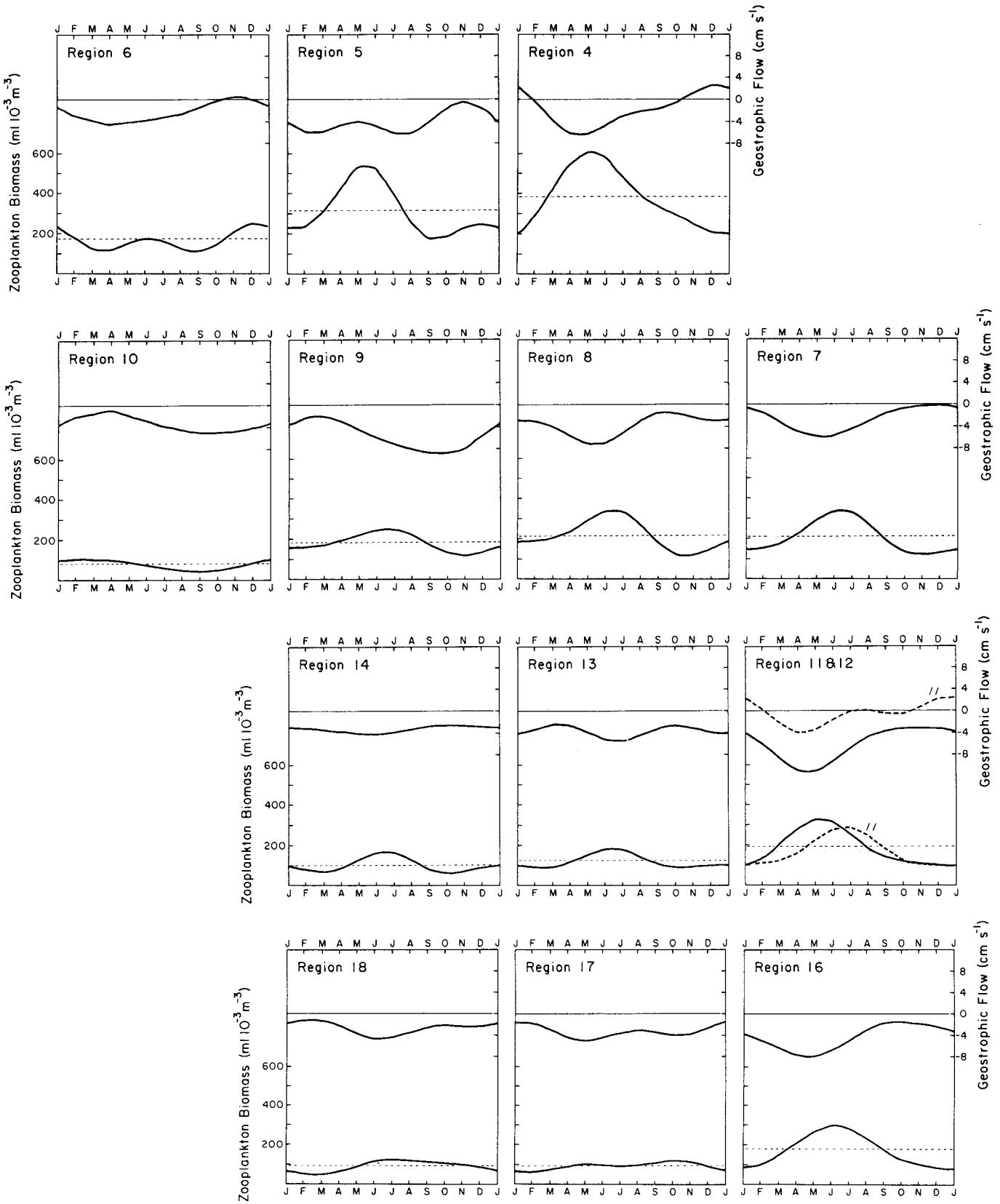

Figure 6. Seasonal cycles of zooplankton displacement volumes (ml/10^{3}m^3) and alongshore geostrophic flow (cm/sec) for each of the 14 zooplankton regions in Figure 4. Seasonal cycles are computed from harmonic analysis of the 32-year record. The mean value of zooplankton is represented by the dotted lines. Graphs are positioned to represent the geographic location of the regions in Figure 4. Regions 11 (*dashed*) and 12 (*solid*) are superposed on the same graph.

upwelling zone, and populations associated with the frontal zone should be confined well within this 50-km boundary. The spatial averaging scheme of this study can only resolve larger-scale fluctuations in offshore populations, since the cross-shore width of the region shown in Figure 4 is 100 km or larger.

Because coastal upwelling is apparently not the impetus behind the large-scale seasonal variability in the offshore zooplankton populations, another driving force must exist. A noteworthy feature of the seasonal zooplankton time series in Figure 6 is the strong presence of semiannual variability in many of the regions. Previous analysis of the seasonal variability of geostrophic flow in the California Current (Hickey 1979; Chelton 1984) has shown that semiannual variability is an energetic component in the seasonal cycle. This suggests a possible causal mechanism for semiannual zooplankton variability. The California Current originates from the West Wind Drift, at approximately 45°N, which comprises mostly subarctic water, rich in both nutrients and zooplankton biomass. Thus variations in transport could result in variations in zooplankton biomass in the California Current.

The seasonal time series of alongshore geostrophic flow are shown in Figure 6 for the 14 zooplankton regions. Careful examination reveals a strong similarity between seasonal variations in alongshore geostrophic flow and zooplankton biomass. With the exception of the four northernmost offshore regions (5, 6, 9, and 10, discussed below), there is a direct correspondence between maxima/minima in zooplankton biomass and maxima/minima in equatorward geostrophic flow. Generally, regions of strong semiannual zooplankton variability coincide with regions of strong semiannual variability of geostrophic flow. In five of the regions (4, 12, 13, 14 and 17), the fluctuations in the cycles of zooplankton and flow are simultaneous. In four regions (7, 8, 16, and 18) changes in zooplankton biomass lag changes in flow by one month. In region 11, changes in zooplankton biomass lag changes in flow by three months.

The high coherence between seasonal cycles of zooplankton and alongshore geostrophic flow is remarkable, particularly in view of the fact that there is regional variation in both the magnitude and timing of the cycles. The springtime maxima of equatorward flow vary by as much as three months from north to south and from nearshore to offshore locations. Secondary winter maxima in equatorward flow become more pronounced in the offshore regions and differ in timing by one or two months in adjacent regions. The magnitudes of the maxima range from 4–12 cm/sec over the CalCOFI domain. These regional variations in the magnitude and timing of seasonal alongshore geostrophic flow are well portrayed in the regional zooplankton cycles.

Two mechanisms have been suggested for observed variations in zooplankton biomass: (1) local zooplankton production in response to nutrient advection and subsequent phytoplankton production, and (2) alongshore advection of zooplankton biomass from northern waters. The time scales of these two processes are quite different. Previous studies of seasonal cycles of nutrient, phytoplankton, and zooplankton concentrations in regions of weak currents (Raymont 1980; Walsh 1977) have found phase lags of two to five months between maximum phytoplankton and zooplankton concentrations, and four to five months between maximum nutrient and zooplankton concentrations. These lags are much longer than the observed lags of zero to one month between zooplankton biomass variations and changes in the alongshore flow. This rapid response is more consistent with advection of zooplankton biomass, which would occur on much shorter time scales, as the dominant mechanism controlling seasonal distributions of zooplankton biomass.

As noted above, seasonal variations in zooplankton biomass and geostrophic flow in the four northern offshore regions (5, 6, 9, and 10) are not as closely coupled as the more nearshore and southern regions. Although the phasing of zooplankton cycles in these regions does not differ notably from the nearshore cycles, the seasonal cycles of the geostrophic flow in these four regions are distinctly different from the seasonal cycles of flow nearer to the coast and to the north and south, both in terms of timing of maximum equatorward flow and in the predominance of the annual or semiannual variability (Figure 6). The alongshore flow along line 70 in region 5 has two maxima in the equatorward transport (February and July) and a single dominant minimum (November). Farther offshore (in region 6) there is a single broad maximum that persists from approximately February through August. Along line 80, just 220 km to the south (in regions 9 and 10), the cycle is quite the opposite, with the maximum equatorward flow occurring in September–October, and the minimum flow occurring in February–March.

This confused picture of seasonal variations in the alongshore component of geostrophic velocity is an artifact of seasonal fluctuations in the speed, location, and orientation of the core of the Califor-

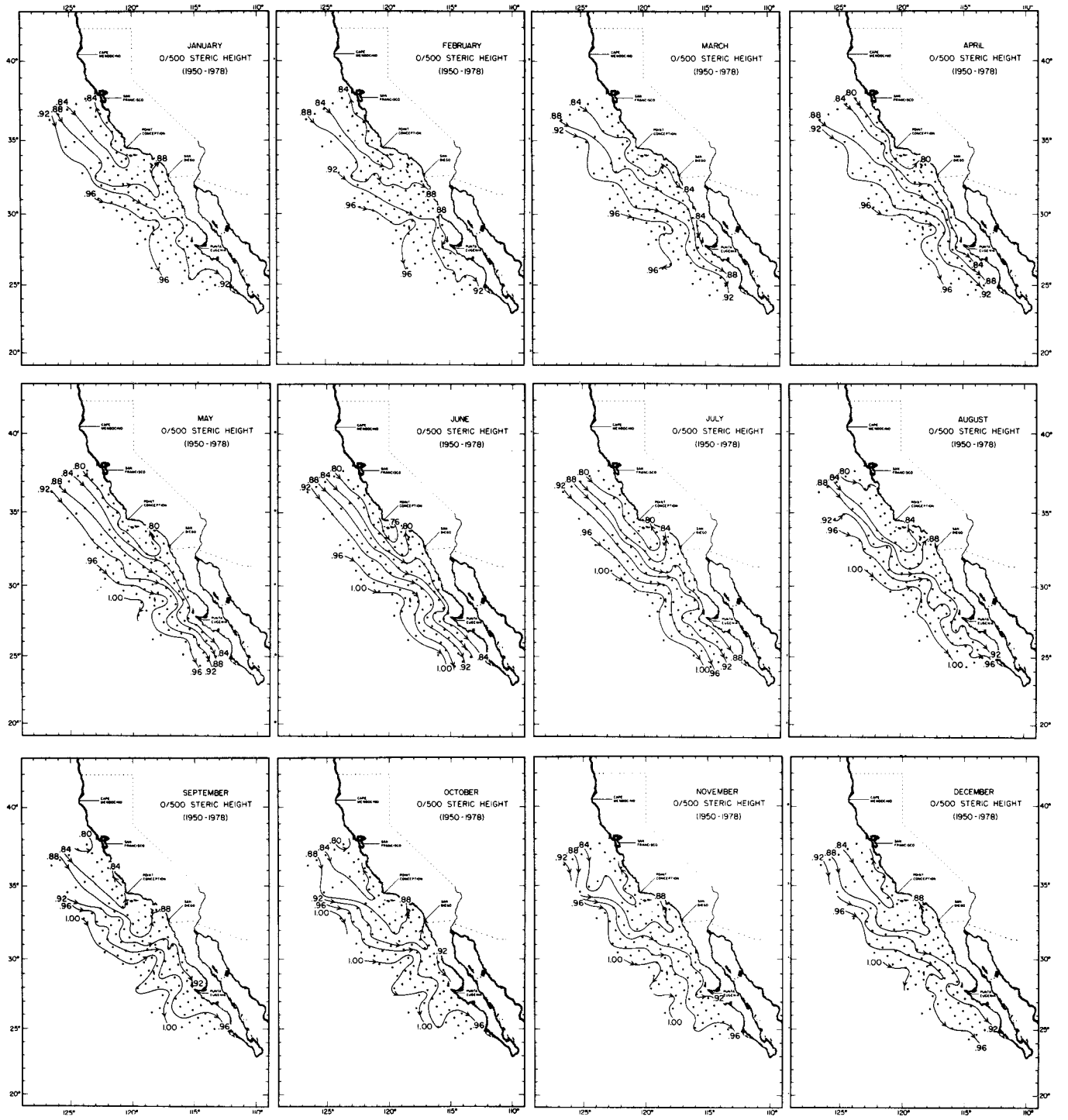

Figure 7a. Contour maps of seasonal mean value of 0/500 db steric height in the CalCOFI survey area. Contour values are in meters, and arrows indicate the direction of geostrophic flow.

nia Current. Meanders in the surface equatorward flow are clearly evident in the contour maps of seasonal steric height (Figure 7a). For comparison, the geostrophic flow at 200 m relative to 500 m is shown in Figure 7b. The quasi-permanent California Undercurrent is apparent in this latter figure. Arrows on the contours in Figure 7a indicate the direction of geostrophic flow, and contour spacing indicates the strength of the flow. From line 70 to line 80, equatorward surface flow is strong in May–July. In August a meander in the surface flow occurs offshore at line 70, introducing a cross-shore

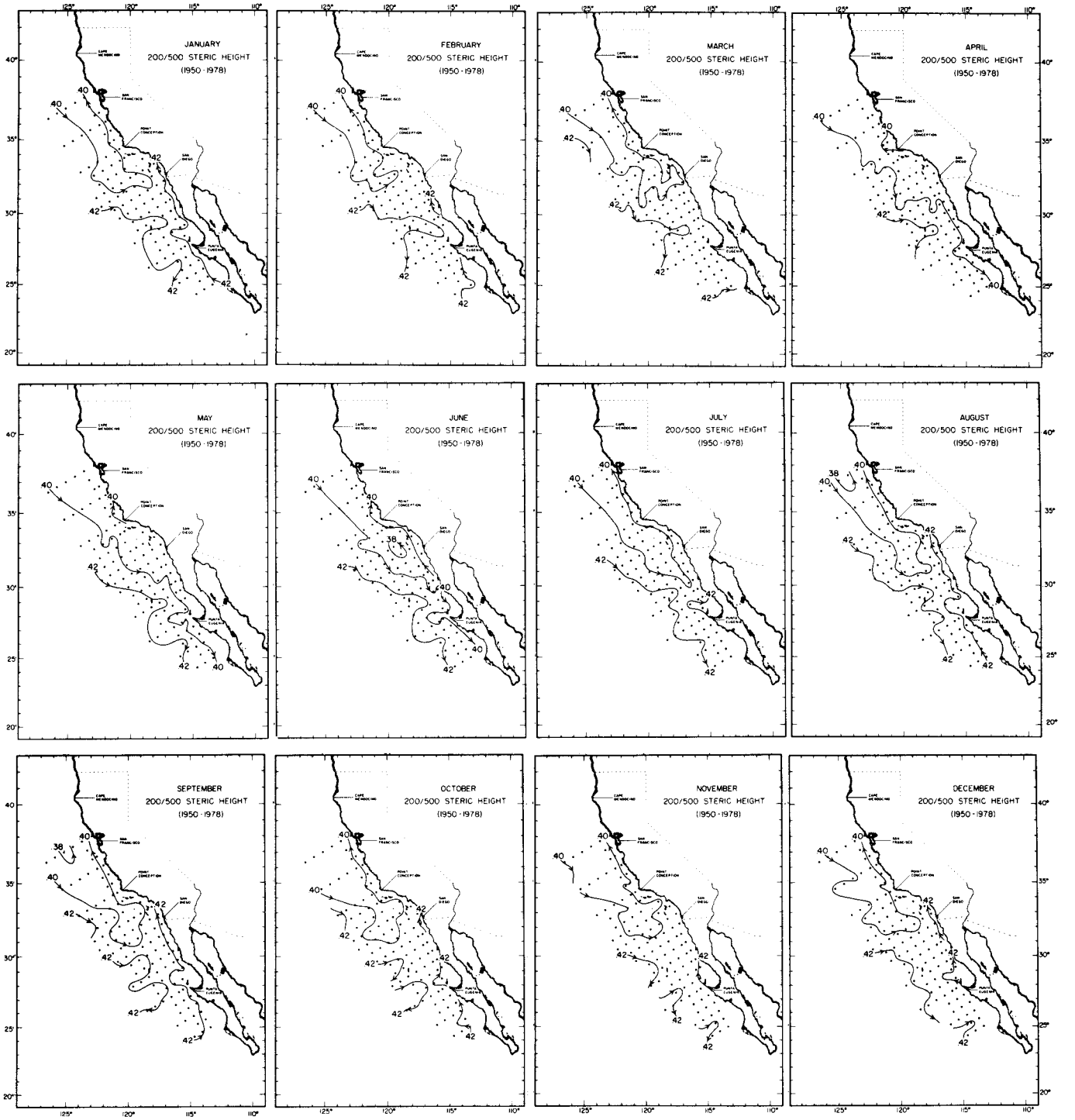

Figure 7b. Contour maps of seasonal mean value of 200/500 db steric height in the CalCOFI survey area. Contour values are in meters, and arrows indicate the direction of geostrophic flow.

component to the flow, and weakened equatorward flow (in regions 5 and 6). The meander persists at this location until December, when it begins to shift southward to line 80. Alongshore surface flow at line 80 (regions 9 and 10) is weak from January to May. The complexity in this region created by the considerable, localized seasonal and spatial variability of the alongshore component of flow may explain the breakdown of the relationship between zooplankton biomass and alongshore geostrophic flow in these four regions. More detailed analyses of both the alongshore and cross-

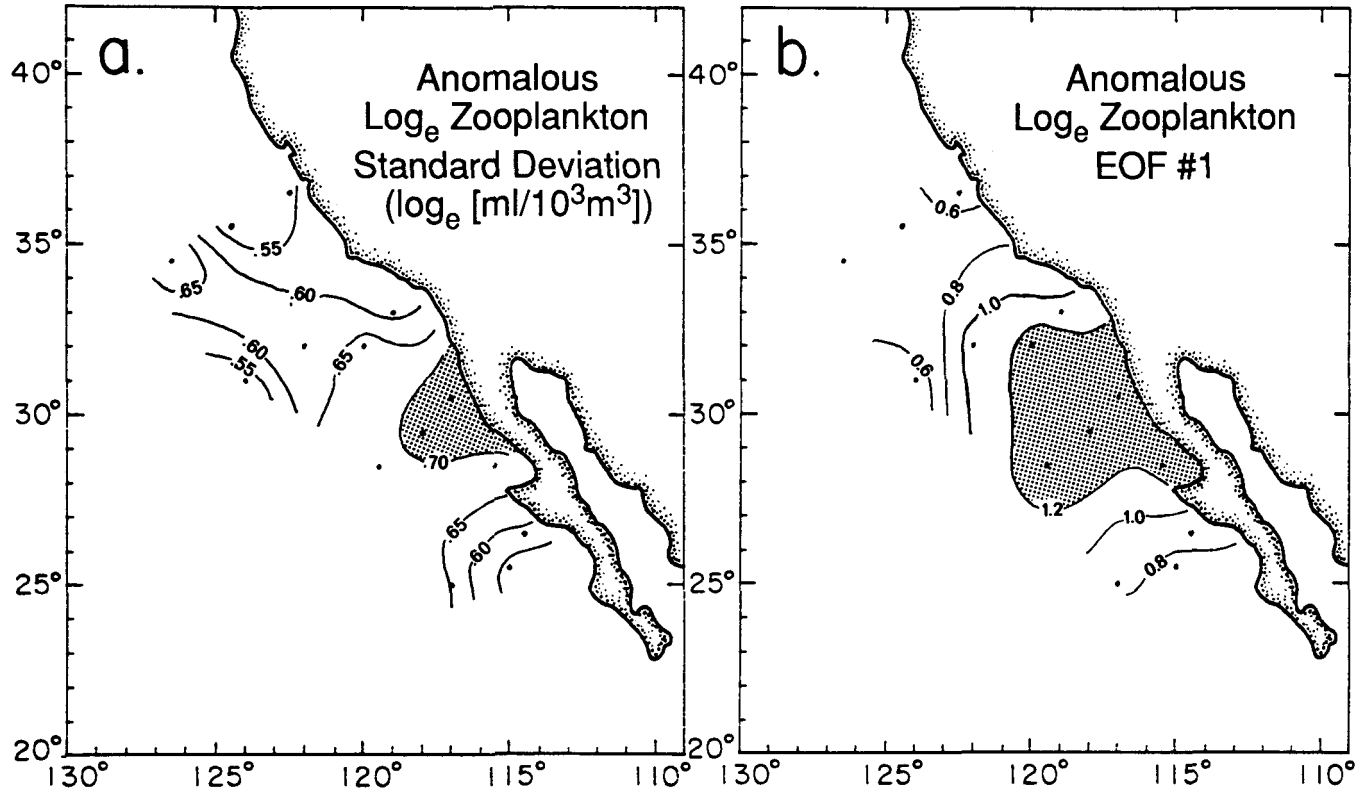

Figure 8. *a*, Standard deviation of $\log_e$ transformed, seasonally corrected zooplankton displacement volumes in the 14 regions denoted by dots. *b*, The dominant EOF of $\log_e$ transformed zooplankton volumes computed over the 14 regions from seasonally corrected time series.

shore components of geostrophic flow may be necessary to understand the seasonal biogeophysical dynamics of this northern offshore area.

NONSEASONAL VARIABILITY

The variance (σ^2) of $\log_e$ transformed, nonseasonal zooplankton volume was calculated for each region by computing the mean of the sum of the squared anomaly values, $z_n(t)$,

$$\sigma^2 = 1/N \sum_{n=1}^{N} z_n^2(t)$$

A contour map of standard deviations (the square root of the variance), Figure 8a, shows that the region of maximum variance is located in a crossshore band approximately 500 km wide in the alongshore direction, near the coast at about 29°N. This band coincides with the biogeographical boundary between high-biomass northern and low-biomass southern species of zooplankton (Bernal 1979; McGowan and Miller 1980). The significance of the coincident bands is discussed later in this section.

Empirical orthogonal functions (EOFs; see Davis 1976) of the $\log_e$ transformed time series were computed. The first-mode EOF (Figure 8b), representing the dominant recurring pattern of spatial variability in the 32-year record, accounts for 49.6% of the total variance. The pattern is strikingly similar to the standard deviation distribution in Figure 8a. Although the standard deviation map in Figure 8a indicates the spatial distribution of variability, it gives no information about the spatial coherence of this variability. The close agreement between the spatial structure of the EOF and the variance distribution indicates that much of the variance in Figure 8a is spatially coherent over the entire CalCOFI region.

The amplitude time series associated with the first EOF of nonseasonal $\log_e$ transformed zooplankton volume (Figure 9c) defines the temporal dependence of the dominant spatial variability. When the time series is positive, there is anomalously high zooplankton biomass throughout the study area; conversely, when the time series is negative, there is anomalously low biomass, with the largest-amplitude fluctuations occurring in the stippled region of high variance in Figure 8b. The EOF amplitude time series is significantly correlated (correlation = 0.94) with the time series of areally averaged zooplankton volume computed by Chel-

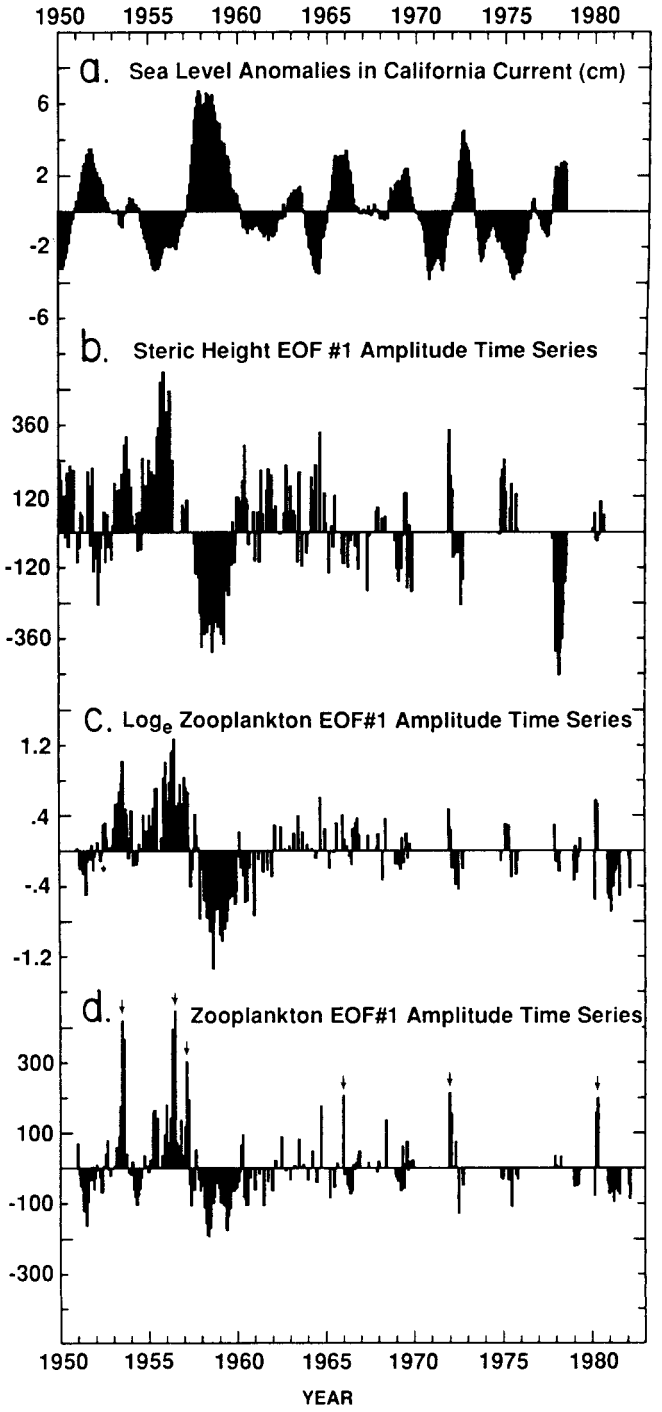

Figure 9. *a*, Time series of sea level anomalies in the California Current (averaged over San Francisco, Los Angeles, and San Diego and corrected for inverse barometric effects of atmospheric pressure) in centimeters. This time series has been smoothed with a double 13-month running average filter. *b*, The amplitude time series of the first EOF of steric height shown in Figure 2b (from Chelton et al. 1982). This time series represents the time dependence of the dominant mode of variability in equatorward advection in the California Current. *c*, The amplitude time series of the dominant EOF of log$_e$ transformed zooplankton displacement volumes shown in Figure 8b. When the time series is positive (negative) zooplankton biomass is anomalously high (low) over the full CalCOFI region (with the largest amplitude variability in the stippled region in Figure 8b). *d*, The amplitude time series for the dominant EOF of untransformed zooplankton displacement volumes. The spatial pattern for this mode is shown in Figure 16b. Arrows indicate the six episodic events discussed in the text.

ton et al. (1982), shown in Figure 1b. This signifies that the large-scale averaging used in that earlier study very effectively draws out the dominant mode of zooplankton variability in the California Current. Figure 8 shows in greater detail how the large-scale variability is distributed spatially. The time-lagged autocorrelation of the amplitude time series of log$_e$ zooplankton (dashed line in Figure 10) indicates a time scale of about 18 months for the dominant signal represented by the first-mode EOF, implying periods on the order of three years.

As noted previously by Chelton et al. (1982), the low-frequency signal in the amplitude time series of the nonseasonal log$_e$ transformed zooplankton is also found in the time series of both sea-level anomalies along the California coast (averaged over San Diego, Los Angeles, and San Francisco) and in the index of southward advection in the California Current (the first-mode EOF of the anomalous steric height). These two time series are shown in Figure 9a and 9b for the 34-year period 1950–83. Cross-correlations between the three time series are statistically significant at better than the 95% confidence level (computed as in Chelton 1982b). Maximum correlations occur when advection lags sea level by three months (correlation = −0.77); log$_e$ zooplankton (EOF amplitude time series) lags advection by two months (correlation = 0.65); and log$_e$ zooplankton lags sea level by five months (correlation = −0.59).

These lagged correlations indicate that, statistically, the order of events begins with an anomalous sea-level signal along the California coast, which

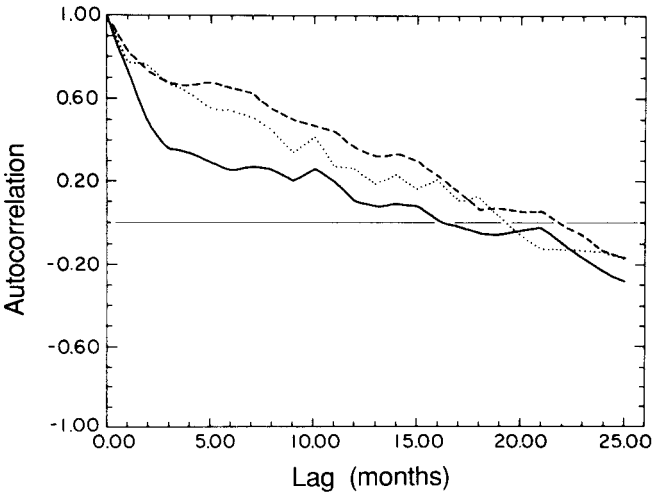

Figure 10. Autocorrelation of the amplitude time series of the dominant EOF of steric height in Figure 9b (*dotted line*); the amplitude time series of the dominant EOF of log$_e$ transformed zooplankton volume in Figure 9c (*dashed line*); and the amplitude time series of the dominant EOF of untransformed zooplankton volume in Figure 9d (*solid line*).

may be transmitted by low-frequency, poleward-propagating, coastally trapped waves (Enfield and Allen 1980; Chelton and Davis 1982). Theoretical arguments and analyses of sea level and current-meter data off the coasts of Oregon (Cutchin and Smith 1973) and central California (Denbo and Allen 1987) suggest that a time period of one to two weeks is required for coastally trapped waves to propagate through the CalCOFI sampling region. In the monthly averages analyzed here, such a propagation of the sea-level anomaly can effectively be taken as an instantaneous event over the CalCOFI sampling region. Three months after the initiation of a positive (negative) sea-level anomaly, equatorward advection in the current is anomalously low (high), followed two months later by anomalously low (high) zooplankton volumes.

From the lagged correlation analysis presented above, it is not possible to unambiguously resolve the biophysical processes linking advection and zooplankton biomass variability. A lag of two months between variations in large-scale zooplankton biomass and advection might be sufficient to account for local zooplankton growth in response to nutrient advection and subsequent phytoplankton production. In this case, the conclusion would be that anomalous advection of nutrients drives anomalous fluctuations in the local zooplankton biomass. Alternatively, the two-month lag between the very-large-scale variability represented by the EOFs of zooplankton and steric height may merely represent the areally averaged response time of local zooplankton abundances to variations in advection of zooplankton biomass. Anomalous fluctuations in biomass analyzed on smaller spatial scales may exhibit regional variations in the lag between variations in advection and zooplankton response. It is undoubtedly true that both processes (advection of nutrients followed by local phytoplankton production and advection of zooplankton biomass) influence zooplankton biomass in the California Current. The challenge is to isolate which, if either, mechanism is dominant.

The EOF analysis presented above describes only simultaneous variations in each of the 14 regions. A regionally varying response time of zooplankton would not be apparent in the EOF analysis. To resolve this type of response it is necessary to examine the relative timings between advection and zooplankton variability on smaller spatial scales. Ideally, a comparison between zooplankton and advection at each of the 14 regions would indicate the precise responses on very small spatial scales. However, the sampling of steric height and zooplankton within each region is too sparse over the 32-year period to accurately resolve the signal of variability on these small spatial scales. It is necessary to average the zooplankton observations over four regions (essentially the same pooled regions previously used by Chelton et al. 1982; see Figure 1a) to investigate regional response of zooplankton biomass to variations in advection. These four areas are indicated by the heavily outlined boxes in Figure 4.

The areally averaged nonseasonal zooplankton time series are shown in Figure 11 for each of the four areas. In area I the time series appears somewhat "noisy." This is due to a combination of biophysical phenomena (this region is highly variable both biologically and physically) and sampling variability (there were fewer surveys of this area than in the more southern areas because of more frequent rough weather). The zooplankton time series for the three southern areas are more "well behaved." The autocorrelation time scales (Figure 12a) of these four time series become progressively longer from north to south, consistent with the results of Chelton et al. (1982).

The lag time between zooplankton biomass fluctuations and alongshore advection is best determined from the phase spectrum in the frequency domain. A simple lagged response is manifested as a linear change in phase with increasing frequency, and the lag time is determined from the slope of the phase spectrum. (For an example of such an application of phase spectra, see Enfield and Allen 1983.) However, the gappy nature of the 32-year CalCOFI time series makes analysis in the frequency domain impossible. The lag time for zooplankton response to advection must therefore be determined from cross-correlations between zooplankton volume and alongshore advection. Because of the inherent long time scales of the nonseasonal $\log_e$ transformed zooplankton volumes and steric height EOF amplitude time series, time-lagged cross-correlations will exhibit broad maxima. It is therefore difficult to ascertain with any statistical reliability the lag of maximum correlation from the gappy time series. Small changes in sample size (adding or removing a few observations) can shift the lag of maximum correlations by a month or two. One must therefore exercise caution when drawing conclusions from lagged correlation analysis.

The cross-correlations between the averaged zooplankton time series for each of the four areas and the index of large-scale advection (the steric height EOF amplitude time series in Figure 9b) are shown

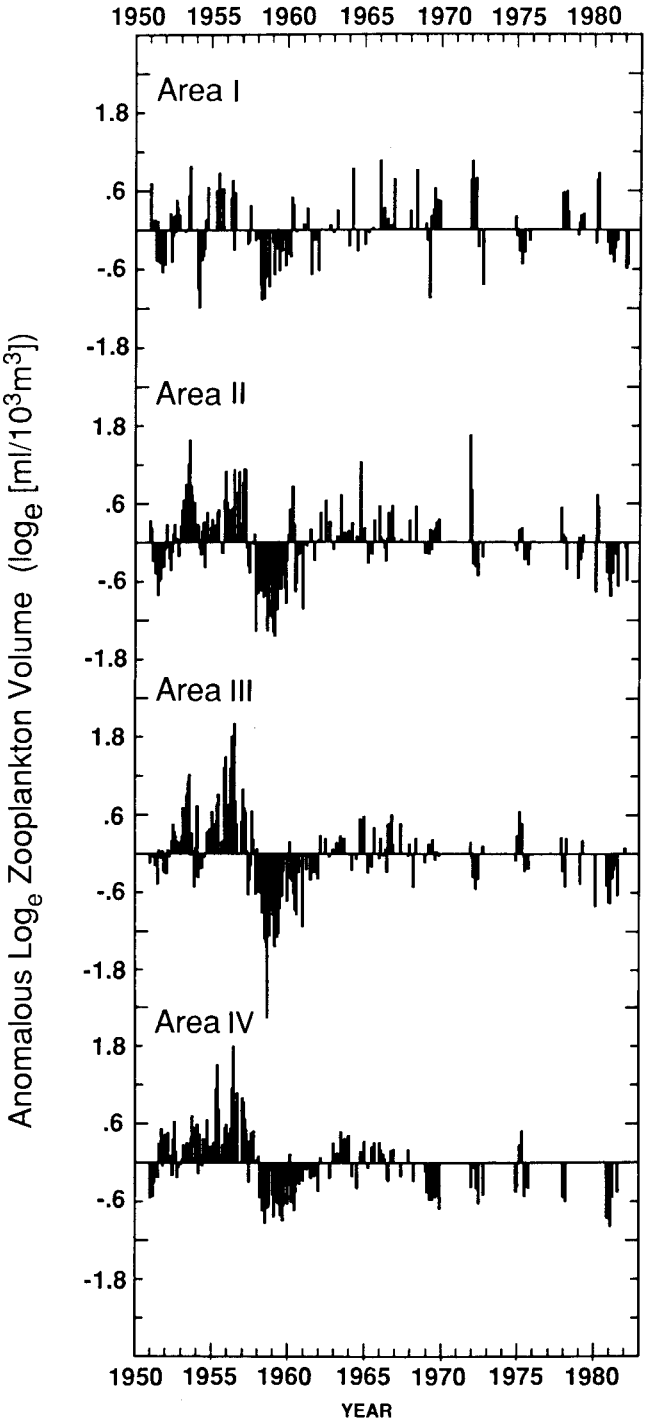

Figure 11. Areally averaged, nonseasonal zooplankton displacement volume time series for the four areas heavily outlined in Figure 4.

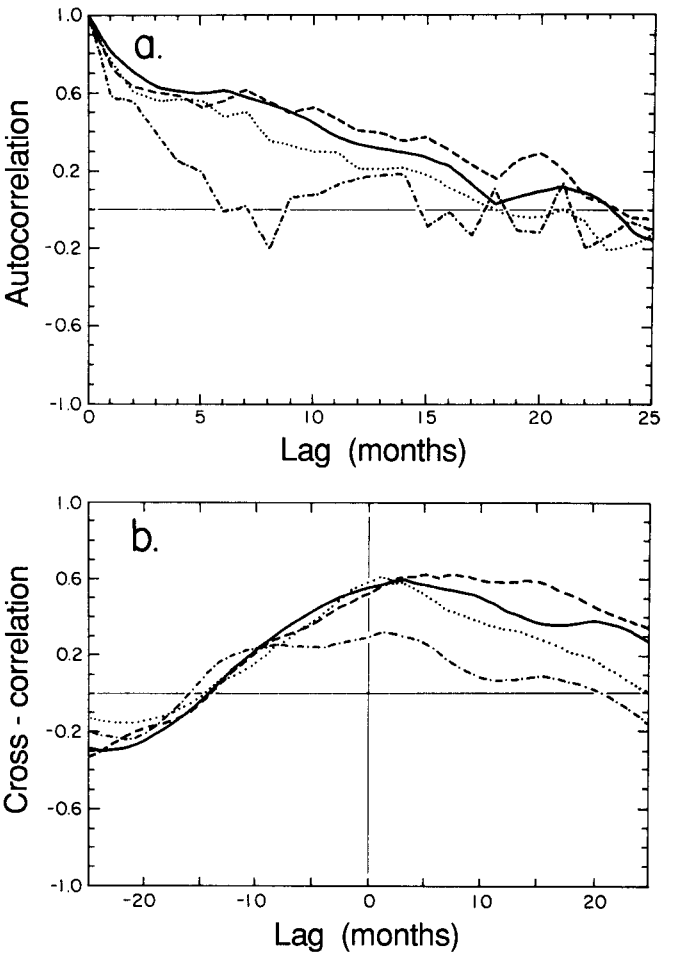

Figure 12. *a*, Autocorrelation of the four areally averaged log$_e$ zooplankton time series (Figure 11) with a dash-dot line for area I, a dotted line for area II, a solid line for area III, and a dashed line for area IV. *b*, Cross-correlation between the four areally averaged zooplankton time series in Figure 11 and the amplitude time series of the dominant EOF of steric height (Figure 9b). The line format convention is the same as that used in *a*.

in Figure 12b. The correlations for areas I and II are maximum when zooplankton biomass lags advection by one month. The lag of maximum correlation becomes progressively longer for areas III and IV (three and five months, respectively). The rapid response time in areas I and II suggests that advection of zooplankton biomass is the dominant mechanism controlling zooplankton abundance in the northern CalCOFI region. The much slower response time in areas III and IV is too long to be explained by simple advection of biomass, suggesting that local zooplankton response to advection of nutrients (followed by phytoplankton production) and to related changes in other environmental conditions (temperature and salinity) is the dominant mechanism controlling zooplankton abundance in the southern CalCOFI region. The shift to longer response time from north to south indicates a shift in importance from advection of zooplankton biomass in the north, to local response to advected environmental conditions in the south.

This relatively simple explanation of the mechanisms controlling zooplankton biomass in the California Current could be somewhat confused if the crustacean component of total zooplankton population is dominated by larval and juvenile stages.

Biomass fluctuations from larval and juvenile growth-rate response to variable food supply are much more rapid than biomass fluctuations from adult reproductive response to variable food supply, because only changes in growth of the individuals and not a complete generation cycle are required to change the total zooplankton volume. It would then be possible that the one-month lag between total zooplankton biomass and advection in areas I and II could be due to larval and juvenile response to advected nutrient concentrations and subsequent phytoplankton production. This mechanism for controlling zooplankton biomass was suggested to us by J.A. McGowan (pers. comm., 1987).

The relative importance of larval and juvenile response to nutrient advection versus advection of total zooplankton biomass can be investigated from maps of larval versus total zooplankton distributions of the genus *Euphausia*. If advection of zooplankton biomass is the primary mechanism governing zooplankton distributions, relatively few established zooplankton (adults and existing juveniles) would be advected equatorward in years of low transport. Most of the zooplankton biomass would result from local new production, and the total zooplankton biomass would be dominated by the larval populations. During years of strong equatorward transport, zooplankton biomass would be dominated by established zooplankton populations, without an increase in productivity, because the biomass is advected equatorward in a water parcel without injection of new food supply. (In fact, the food supply within the parcel of water would decrease with time, as the nutrients were consumed by phytoplankton.) In this case, larval populations would account for a small fraction of the total biomass.

Larval and total zooplankton distributions of *E. pacifica* have been published by Brinton (1967) for 1955 and 1958. Distributions during April (Figure 13a), when zooplankton biomass and equatorward flow are normally high, indicate that year-to-year variations in larval versus adult dominance in response to advection are important in the northern CalCOFI region. During 1955 (a year of strong equatorward advection) the distribution of *E. pacifica* was dominated by adult populations. During 1958 (a year of weak equatorward advection), the *E. pacifica* populations were dominated by larval stages. If these examples are typical for the subarctic species, years of strong equatorward transport are characterized by a dominance of adult populations, and years of weak equatorward transport are characterized by dominance of larval stages of local populations of subarctic species. This is consistent with the interpretation that advection of zooplankton biomass is the dominant mechanism controlling zooplankton abundance in the northern CalCOFI region.

Distributions of larval and total zooplankton biomass of the subtropical euphausiid *E. eximia* during years of strong and weak equatorward advection are very different from the subarctic species (Figure 13b). The populations are dominated by larval stages in both years. Clearly, some other mechanism must be controlling zooplankton biomass in the southern CalCOFI region. Phytoplankton (and hence zooplankton) productivity are more nutrient-limited in the southern half of the CalCOFI domain than in the north. When food supply is low (periods of weak equatorward advection) zooplankton biomass will be dominated by larval and juvenile stages. Input of higher food supply during years of strong equatorward advection would lead to local new production, which also results in a dominance of larval populations in the total zooplankton biomass. Assuming that these distributions of larval versus total zooplankton biomass are typical of subtropical species and representative of years of strong and weak advection, the observed zooplankton variability in the southern CalCOFI region is consistent with the hypothesis that local zooplankton response to advection of nutrients and changes in environmental conditions is the dominant mechanism controlling nonseasonal zooplankton abundances. This result is intuitively sensible: equatorward advection of biomass cannot increase the abundances of the subtropical species in this region because, unlike subarctic species, subtropical species decrease in abundance from south to north.

As noted previously, the region of largest variability of nonseasonal zooplankton biomass (Figure 8a) coincides with the region of transition from subarctic to subtropical species. This suggests that the dominant variability of total zooplankton biomass may be due to simple meridional migrations of biogeographical boundaries (defined here to be the region of strongest gradients in zooplankton biomass). Our premise that the processes controlling zooplankton abundance are advection of zooplankton biomass in the northern area and local zooplankton response to advection of nutrients and changes in environmental conditions in the southern areas can be further investigated by examining the locations of the biogeographical boundaries of subarctic and subtropical zooplankton populations during years of anomalously high

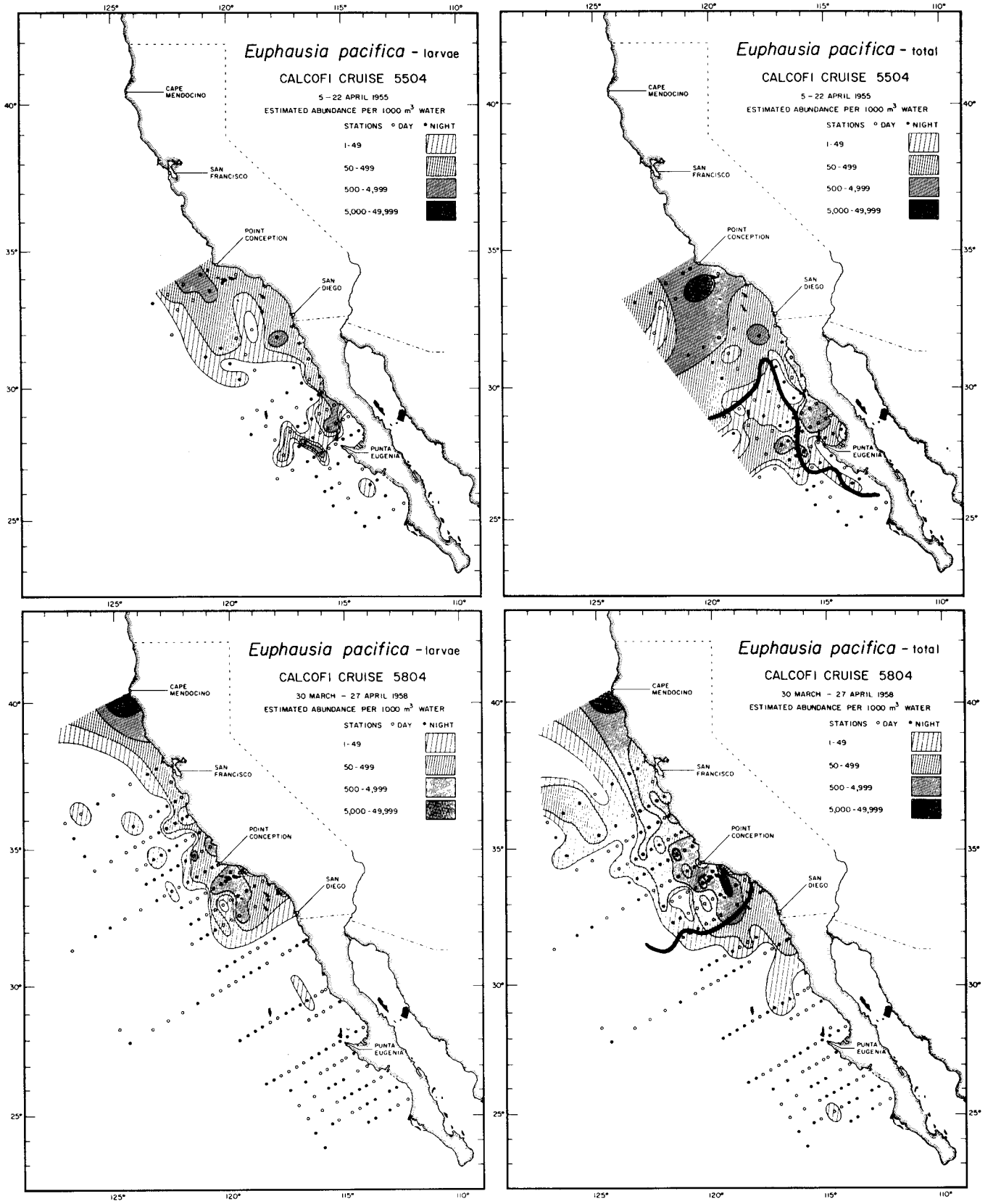

Figure 13a. Larval versus total zooplankton distribution of *Euphausia pacifica*, a subarctic species, for April 1955, an anomalously cold year, and April 1958, an anomalously warm year (Brinton 1967). The black line on the total distributions indicates the approximate location of the 15.5°C isotherm for each date (Anonymous 1963).

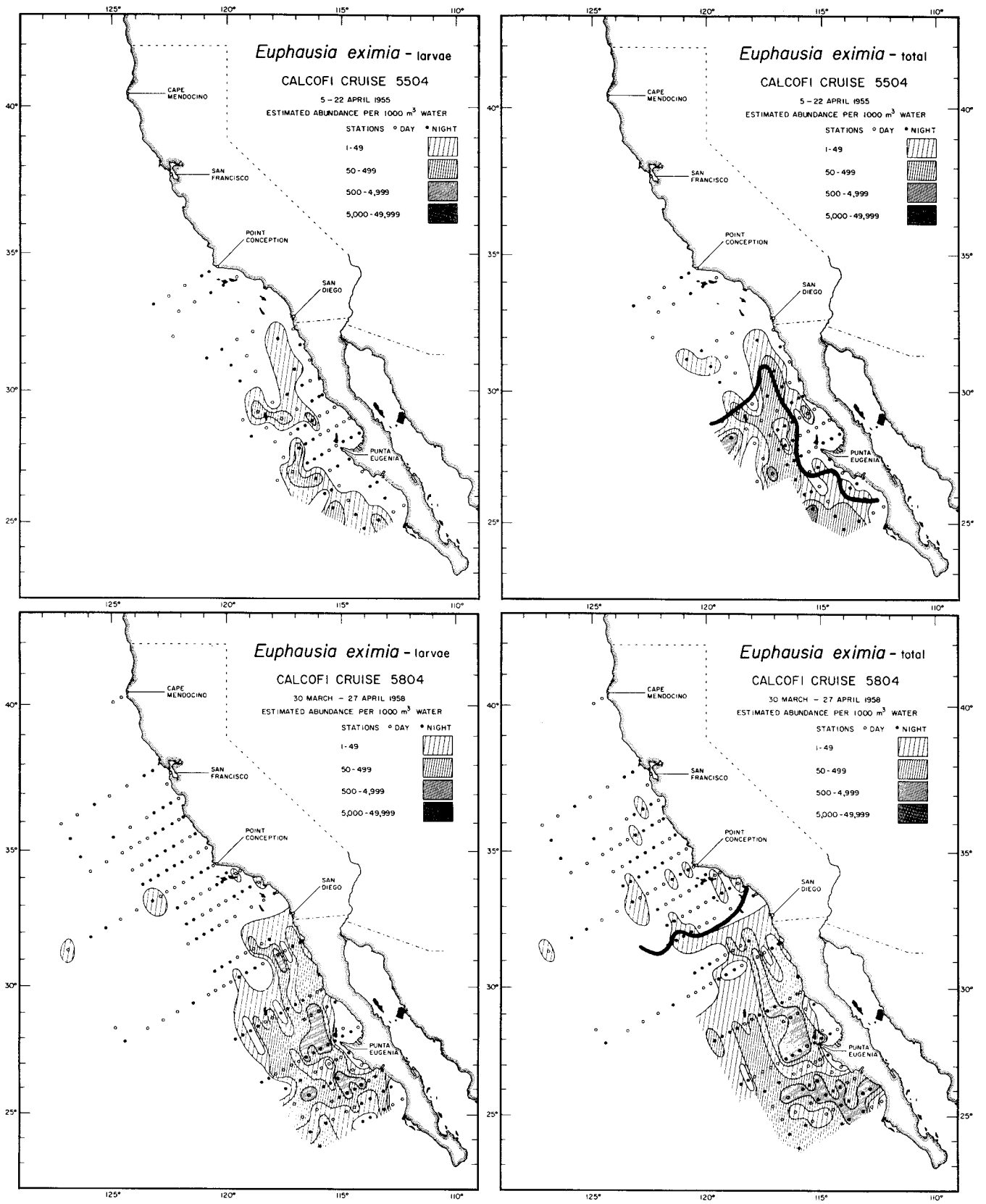

Figure 13b. Larval versus total zooplankton distribution of *Euphausia eximia*, a subtropical species, for April 1955, an anomalously cold year, and April 1958, an anomalously warm year (Brinton 1967). The black line on the total distributions indicates the approximate location of the 15.5°C isotherm for each date (Anonymous 1963).

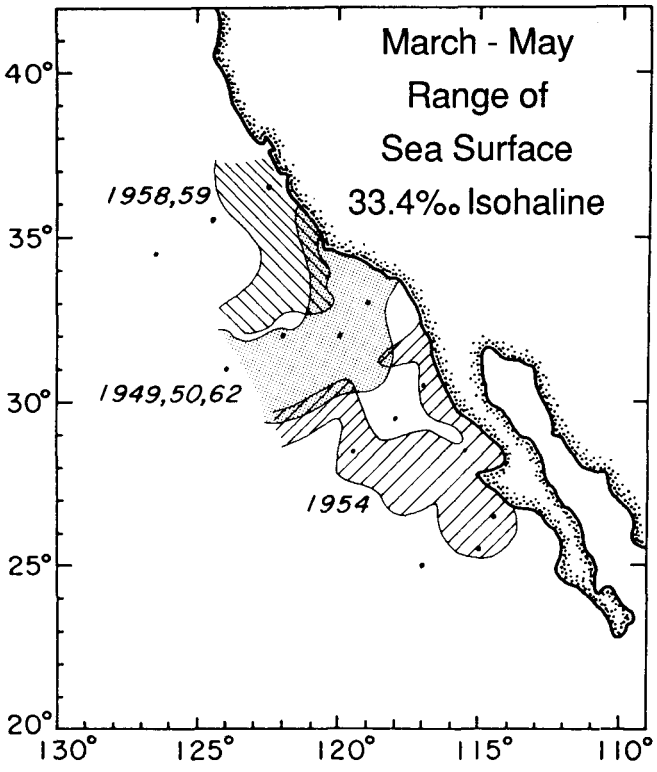

Figure 14. March-through-May averaged range of the sea-surface 33.4‰ isohaline in the CalCOFI survey area for cold years (1949, 1950, 1954, and 1962) typified by strong equatorward transport of subarctic water, and warm years (1958 and 1959) typified by weak equatorward transport. (Data taken from Wyllie and Lynn 1971.)

and low transport. High equatorward transport (positive values in the EOF amplitude time series of steric height, Figure 9b) is characterized by an insurgence of cold, low-salinity subarctic water, rich in nutrients and populated by transition-zone and subarctic zooplankton species (Bernal 1979). Low equatorward transport (negative values in the steric height EOF amplitude time series) is characterized by decreased equatorward advection of cold, low-salinity subarctic water, and in some cases, a reversal in the normal equatorward flow of the California Current resulting in poleward advection of equatorial water, higher in temperature and salinity, lower in nutrient concentrations, and inhabited by subtropical zooplankton species (Bernal 1979).

As noted in the Introduction, Bernal (1979, 1981) and Bernal and McGowan (1981) have identified the 33.4‰ isohaline as the boundary separating the subarctic and subtropical water masses. The location of this isohaline can thus be used to identify year-to-year variations in the equatorward penetration of the subarctic water mass. The range of positions of the 33.4‰ isohaline for March through May of years with weak (1958 and 1959) and strong (1949, 1950, 1954, and 1962) equatorward transport is shown in Figure 14. (These years coincide with years for which maps of zooplankton abundance distributions have been previously published: see discussion below.) The water mass boundary shifts north and south with changes in equatorward transport of the California Current.

The distributions of total biomass of the subarctic species *E. pacifica* and the subtropical species *E. eximia* are shown for April 1955 and 1958 in Figures 13a and 13b (Brinton 1967). These correspond to anomalously cold and warm years, characterized by anomalously weak and strong equatorward advection (see Figure 9b). The dark line on each map indicates the approximate location of the 15.5°C isotherm for each year (Anonymous 1963). As expected, the location of this isotherm fluctuates north and south depending on the strength of advection in the California Current. It is evident from Figures 13a and b that the biogeographic boundaries of both the subarctic and the subtropical species of euphausiids migrate north and south synchronously with the isotherm. Maps of distributions for other dominant species in the CalCOFI region are shown in Appendix 2 for years of weak and strong equatorward advection in the California Current. They show the same patterns of meridional biogeographic boundary migrations that are seen in Figure 13a for *E. pacifica* and 13b for *E. eximia*.

Equatorward shifts in the boundary of the northern transition and subarctic species occur during years of anomalously strong equatorward advection. Similarly, poleward shifts occur during years of weak equatorward advection. As noted previously, the time lag between zooplankton biomass and equatorward advection is short (one month) in areas I and II (Figure 12b). The boundary shifts, synchronous with changes in advection, and the rapid response of zooplankton biomass to advection are all consistent with the interpretation that advection of zooplankton biomass is the dominant mechanism controlling zooplankton variability in the northern half of the CalCOFI domain.

Figures 13a, 13b, and the figures in Appendix 2 show that the biogeographical boundaries of southern species of zooplankton also move north and south in response to changes in alongshore advection. Equatorward shifts in boundary location associated with increased advection could be interpreted as alongshore advection of zooplankton biomass (as in the northern regions). However, northward shifts of the subtropical species' boundary locations during periods of weak equatorward advection are more difficult to explain by simple

advection of zooplankton biomass. This mechanism requires actual reversals of the normally equatorward flow south of 32°N (see Figure 7a) in order to advect southern species northward. Such reversals do occur near the coast (within 100–200 km) during highly anomalous years (Wyllie 1966) but are not general broadscale features when the equatorward advection index in Figure 9b is negative. Another possible mechanism for northward advection of subtropical zooplankton biomass is the poleward undercurrent present throughout the year at depths greater than 100–150 m (see Figure 7b). Wroblewski (1982) has suggested a mechanism by which the undercurrent can control the alongshore position of zooplankton. Adult copepods are known to undertake diel vertical migrations to depths exceeding 200 m (Brinton 1962). During years of weak equatorward transport in the near-surface waters, these diel vertical migrations could result in net northward advection of subtropical species.

From the discussion above, it is tempting to explain the observed meridional shifts in location of subtropical zooplankton species boundaries by simple advection of zooplankton biomass, similar to the mechanism proposed for the subarctic species. However, this interpretation is inconsistent with the lagged correlation analysis in Figure 12b, which implies a long response time (three to five months) between zooplankton biomass and alongshore advection in areas III and IV. This lag is too long to be explained by simple advection of zooplankton biomass. From the maps of zooplankton distributions in Figure 13 and Appendix 2, it is evident that isolated populations of subtropical species of zooplankton are always found north of the biogeographical boundary of the species (as defined by the region of strong gradient from high to low abundance). However, these isolated populations are sparse and consist of relatively low biomass, presumably because of unfavorable environmental conditions. Weakened equatorward transport results in a northward shift of the high temperature and salinity usually associated with southern waters and subtropical zooplankton species. Northward shifts of subtropical species boundaries during periods of weak equatorward transport could therefore represent blooms of these isolated populations in response to more favorable conditions for the subtropical species farther north. Such a mechanism for controlling zooplankton biomass would account for the observed slower response (three to five months) of zooplankton to changes in advection in areas III and IV.

From Figure 13 and the figures in Appendix 2, it is apparent that the region of high zooplankton variability in Figure 8a does indeed represent meridional shifts in subarctic and subtropical species boundaries. Geographical fluctuation of the southern boundary of the subarctic water mass and its associated groups of zooplankton defines the spatial structure of the dominant EOF of nonseasonal, $\log_e$ transformed zooplankton biomass (Figure 8b). This is consistent with the results of McGowan and Miller (1980). In the northern CalCOFI region they found low diversity and high species dominance by subarctic and transition species. They found low diversity and high species dominance by subtropical species in the southern CalCOFI region. In the region that we have identified as the highly variable zone inhabited by both zooplankton groups, they found high diversity and low species dominance.

We conclude that the low-frequency signal in zooplankton biomass is closely related to variability in the equatorward advection of the California Current, as previously pointed out by Chelton et al. (1982). It appears that these zooplankton fluctuations are not solely local responses to changes in nutrient advection, as hypothesized in the earlier study. The timing of the low-frequency zooplankton response to advection inferred from lagged correlation analysis indicates that both advection of zooplankton biomass and local zooplankton response to advection of nutrients and changes in environmental conditions drive the variability of zooplankton biomass in the California Current system. In the northern regions, advection of biomass seems to be the dominant process. In the southern regions, it appears that zooplankton biomass is dominated by local responses of zooplankton to advection.

HIGH-FREQUENCY NONSEASONAL VARIABILITY

As noted previously, zooplankton data are generally $\log_e$ transformed before analysis. In part, this is to reduce or eliminate spikes in the zooplankton time series; the spikes are often believed to be due to sampling variability from patchiness in the spatial distribution of zooplankton biomass. As an example, the time series of seasonally corrected raw zooplankton volumes and $\log_e$ transformed zooplankton volumes for region 8 are shown in Figure 15. Note the underlying similarity in the low-frequency aspects of variability. Also note the spikes in the raw zooplankton time series that do not appear in the $\log_e$ transformed data.

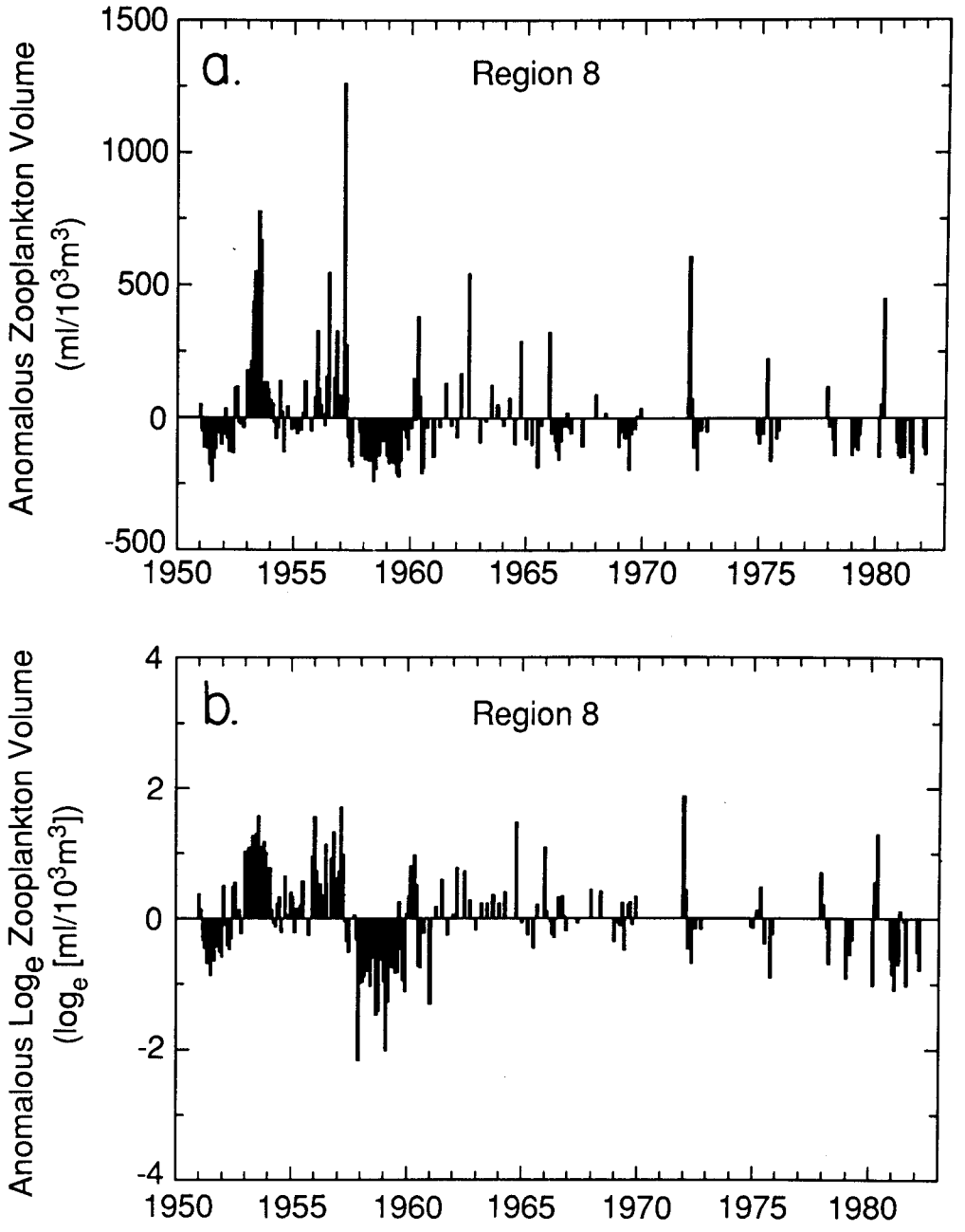

Figure 15. *a*, Seasonally corrected zooplankton displacement volume time series for region 8. Note the episodes of exceptionally high biomass superimposed upon the underlying low-frequency signal. *b*, Seasonally corrected $\log_e$ transformed zooplankton displacement volume time series for region 8. Note the dominant low-frequency variability as seen in the previous time series, and the absence of the episodic signals.

Careful inspection of Figure 15a shows that these energetic pulses often have time scales of two to four months (e.g., June–August 1953; May–July 1956; March and April 1957; January and February 1972; and April and May 1980). This implies that, rather than being spurious data points resulting from sampling variability, these spikes probably represent important physical and biological processes. The raw (untransformed) zooplankton data are analyzed in this section to investigate the nature of these episodic events in zooplankton biomass.

A contour map of the standard deviation of untransformed data is shown in Figure 16a. The spatial structure is surprisingly different from the standard deviation map of $\log_e$ transformed zooplankton (Figure 8a). Rather than the local concentration of variability at the biogeographical boundary separating northern and southern zooplankton species in the transformed data, the spatial structure of untransformed zooplankton variability consists of a tongue extending from the northern regions southward to approximately 27°N. Evidently, there are physicial and biological

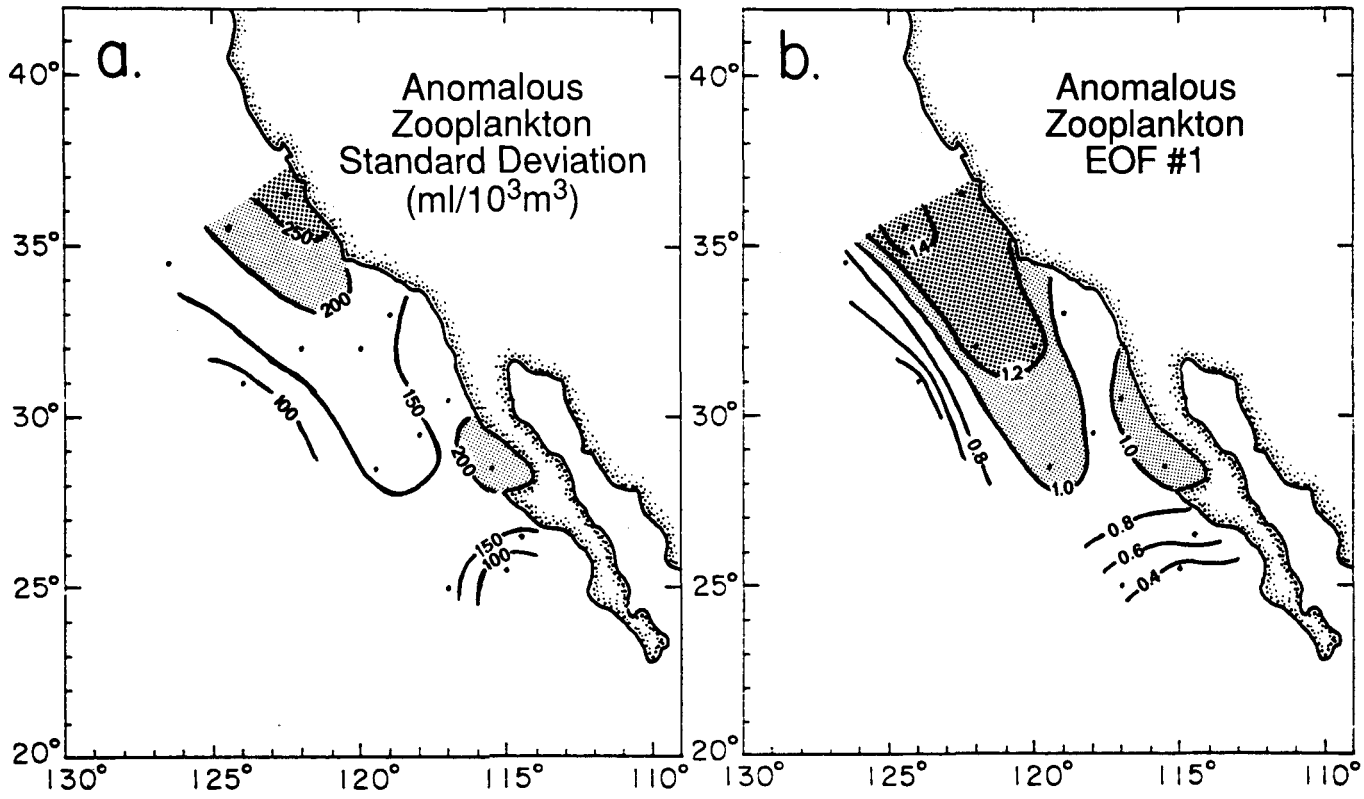

Figure 16. *a*, Standard deviation of the seasonally corrected untransformed zooplankton displacement volumes over the 14 regions. *b*, The dominant EOF of untransformed zooplankton displacement volumes over the 14 regions. When the amplitude time series (in Figure 9d) is positive (negative), anomalously high (low) biomass occurs over the full CalCOFI region, with the largest amplitude fluctuations occurring in the stippled regions.

processes that appear in the untransformed zooplankton volumes but not in the $\log_e$ transformed zooplankton volumes.

The dominant EOF of untransformed zooplankton volume is shown in Figure 16b. It is apparent from this EOF pattern that the variability shown in Figure 16a is spatially coherent over the CalCOFI domain. The spatial structure of untransformed zooplankton variability is very different from that of the $\log_e$ transformed zooplankton variability. The effects of noise in time series of zooplankton biomass on the spatial structure of EOFs are discussed in detail in Appendix 1. It is shown that the spatial EOF pattern is unaffected by spatially and temporally random spikes in the time series. Thus the differences between the first EOFs of $\log_e$ transformed and untransformed zooplankton volumes must be attributable to the spikes in the untransformed data, and these spikes must be coherent spatially. This is an important conclusion, for it implies that the pulses of biomass in Figure 15a are not spurious data points. The spatial structure of these variations in untransformed zooplankton biomass indicates a northern origin extending equatorward as far south as about 27°N in a tongue approximately 600 km long, with the region of highest variability centered about 350 km offshore in the southern region. An important point to note is that the EOF pattern represents spatially coherent pulses of zooplankton biomass along the axis of the tongue. That is, the pulses of zooplankton biomass are evidently not random in space and time, but rather are a relatively large-scale process.

The amplitude time series of the first EOF of untransformed nonseasonal zooplankton volume is shown in Figure 9d. Over the period 1951–82, six large-scale pulses of zooplankton biomass were observed with magnitudes exceeding 200 ml/10³m³ (indicated by arrows in the EOF amplitude time series). All six of these episodic events occurred between January and June and persisted for two to three months. That is, these anomalous large-scale features in zooplankton biomass, observed in the untransformed zooplankton volumes on two to three consecutive CalCOFI cruises, are not spurious data points. The time-lagged autocorrelation of the untransformed zooplankton EOF amplitude time series is shown as the solid line in Figure 10. The zero crossing at large lag (16 months) indicates an underlying low-frequency signal in the untrans-

formed zooplankton variability. The rapid drop in autocorrelation from zero lag to three months indicates the short (two-to-three-month) time scale associated with episodic events. The dominant EOF of untransformed nonseasonal zooplankton variability thus represents two separate biophysical processes.

In the California Current, total zooplankton volume is sometimes dominated by large gelatinous zooplankton (Berner 1967). A bloom of gelatinous zooplankton, known to have doubling times on the order of weeks (Mark Ohman, pers. comm., 1986), would certainly skew a total zooplankton displacement volume count because of the larger size of the individuals. We examined all of the published maps of Thaliacea (salp) distributions (Berner 1967). There are no published maps concurrent with any of the six large-scale episodic zooplankton events in Figure 9d, so it is not possible to say definitely whether these pulses represent blooms of all components of total zooplankton volume or blooms of only the gelatinous zooplankton. However, from published maps at times when anomalous blooms of Thaliacea did occur, values of the untransformed, nonseasonal zooplankton volume amplitude time series did not exceed 100 ml/10^3m^3. (Anomalously large abundances of Thaliacea were observed for the following species: *Dolioletta gegenbauri* on CalCOFI cruises 5106, 5206, 5209, and 5806; *Cyclosalpa bakeri* on cruise 5111; *Salpa fusiformis* on cruises 5203 and 5404; and *Thalia democratica* on cruises 5109, 5110, 5111, 5206, and 5804.) It is therefore unlikely that the six observed large-scale pulses of zooplankton biomass are the result of a bloom of only the gelatinous zooplankton. An examination of the zooplankton volumes collected during the six episodic zooplankton events is necessary to ascertain this conclusively.

We have been unable to resolve the mechanism responsible for the generation of these episodic events in zooplankton biomass. They are not significantly correlated with the index of advection in the California Current, wind stress curl over the region, or horizontal shear in the alongshore flow (as defined by the second EOF of steric height; Chelton 1982a). One possible process that could produce the observed pulses in zooplankton biomass is the injection of coastal water, rich in nutrients and phytoplankton, into the California Current by coastal filaments or jets, which have been frequently observed off the California coast (e.g., Tragazna et al. 1981; Kosro 1987; Chelton et al. 1987; Abbott and Zion 1987; Mooers and Robinson 1984). Local zooplankton populations responding to the resultant ideal feeding conditions would be expected to increase relatively rapidly. Subsequent detachment of the filaments, possibly in the form of cold-core rings (e.g., Haury 1984; Simpson 1984; Haury et al. 1986), results in separation from the coastal source of nutrients. As the detached coastal filaments are advected equatorward by the California Current, rapid uptake by phytoplankton populations would diminish the nutrient concentrations so phytoplankton production, followed by zooplankton production, would subsequently crash because of consumption of the limited food supply. The original lower abundances of zooplankton would then be restored on a time scale of one to three months.

Filaments originating off Cape Blanco, Point Arena, and Cape Mendocino (Kosro 1987; Kosro and Huyer 1986) could account for zooplankton events that appear to originate offshore in the northern regions. Filaments off Monterey and Point Conception (Traganza et al. 1981; Atkinson et al. 1986; Chelton et al. 1987; Abbott and Zion 1987) could account for events originating off the central and southern California coast. The characteristics of detached filaments (duration, location, and extent into the current) would determine the fate of the isolated zooplankton populations.

This hypothesis can be tested with historical satellite-derived estimates of phytoplankton biomass inferred from surface chlorophyll concentrations estimated from ocean color measurements by the Coastal Zone Color Scanner (CZCS), and sea-surface temperature measurement by the Advanced Very High Resolution Radiometer (AVHRR). Pelaez and McGowan (1986) have analyzed patterns of seasonal development from selected CZCS and AVHRR images of the California Current region from July 1979 to April 1982. One of these sequences coincides with an observed pulse of zooplankton biomass in April and May of 1980 (Figure 17). A CZCS image from February 7, 1980, shows three fully developed rings located 400–500 km offshore. Three additional rings appear to be in the process of forming from filaments off Monterey, Point Conception, and San Diego (Pelaez and McGowan 1986). The locations of these rings and filaments are superimposed as stippled patterns on the zooplankton distribution for April and May 1980. In April, the high zooplankton biomass in the northern CalCOFI region coincides with the location of the large filament off Monterey. In May, the zooplankton biomass is highest off Monterey, and there is a tongue of high zooplankton biomass located 150 km offshore extending south-

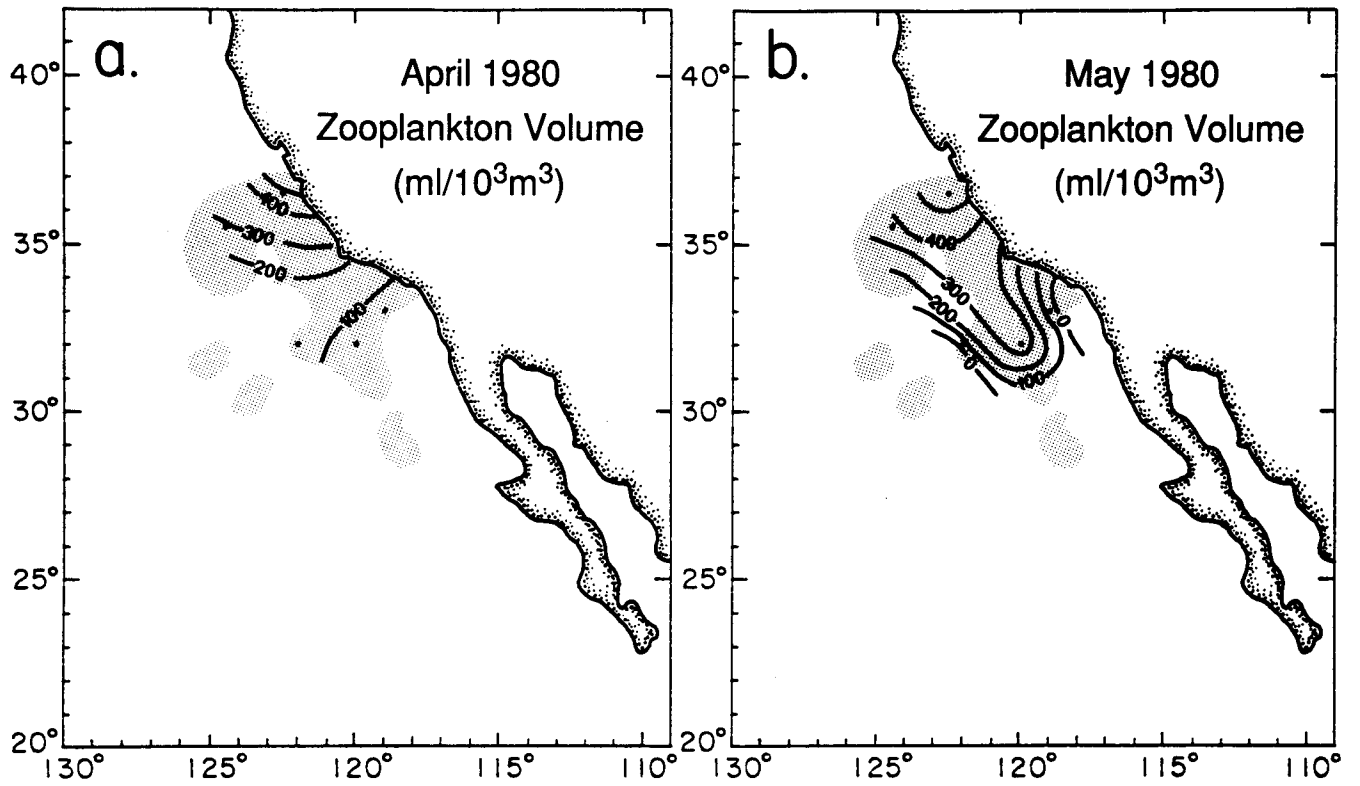

Figure 17. The anomalous zooplankton distributions for the pulse event in April and May of 1980. Contour lines are in intervals of 100 ml/10^3m^3. The stippled pattern indicates the location of the developing rings located on the February 7, 1980, CZCS image (from Pelaez and McGowan 1986).

ward at least as far as 31°N. (The May 1980 CalCOFI cruise did not sample the region farther south.) When two months' lag is allowed for zooplankton to respond to increased phytoplankton and nutrient input in the offshore waters, the relationship between zooplankton and coastal filaments of high phytoplankton concentration appears to be strong.

CONCLUSIONS

Analysis of the 32-year CalCOFI record of zooplankton displacement volumes has identified recurring patterns of variability. Seasonal variability of large-scale zooplankton biomass appears to be predominantly controlled by advection of zooplankton biomass over most of the CalCOFI sample region. The co-occurrence of maxima (minima) of zooplankton biomass with maxima (minima) of equatorward geostrophic flow in the seasonal cycles does not allow sufficient lag time for zooplankton response to changes in nutrient input from advection.

Nonseasonal variability of $\log_e$ transformed zooplankton volume is dominated by a very-low-frequency signal, with periods of three to five years associated with variations in large-scale equatorward transport in the California Current. In the northern half of the CalCOFI domain, the biogeographical boundaries of subarctic species of zooplankton shift north and south synchronously with variations in alongshore transport, and the response of zooplankton biomass to advection is rapid (one-month time lag). The total zooplankton biomass is dominated by adult stages during periods of strong equatorward advection and by larval stages during periods of weak equatorward advection. This evidence is all consistent with an interpretation that alongshore advection of zooplankton biomass is the dominant mechanism controlling zooplankton abundance in the northern CalCOFI region.

The behavior of subtropical species of zooplankton in the southern half of the CalCOFI domain is fundamentally different. The time scales of variability are much longer, and the biomass appears to be always dominated by larval and juvenile stages. The biogeographical boundaries of subtropical species migrate north and south in response to changes in alongshore advection, but the response time is much longer (three to five months) than in the northern regions. This evidence is more consistent with an interpretation that zooplankton

abundance is controlled by local biomass response to changes in environmental conditions associated with changes in alongshore advection.

Intuitively, this explanation for the relation between advection and zooplankton biomass is appealing. In the northern CalCOFI region, the food supply for zooplankton is plentiful (high nutrient and phytoplankton concentrations). Consequently, the zooplankton populations thrive and are not generally food-limited. Then changes in alongshore advection simply transport the biomass distributions. In the southern CalCOFI region, the nutrient (and therefore phytoplankton) concentrations are generally much lower (except very near the coast, where upwelling is important). Since the food supply is less plentiful, adult stages of subtropical zooplankton are less populous, and the biomass is dominated by larval stages. Abundances of subtropical zooplankton species decrease northward, so increased equatorward advection does not increase zooplankton abundance by simple advection of zooplankton biomass. The subtropical zooplankton populations are more sensitive to changes in environmental conditions (increased nutrient supply during periods of strong equatorward advection, and more favorable temperature and salinity conditions during periods of weak equatorward advection).

Analysis of non-$\log_e$ transformed zooplankton volumes reveals a second, higher-frequency signal in nonseasonal zooplankton variability, which is lost in the $\log_e$ transformation. Episodic bursts of zooplankton biomass with durations of three to four months have occurred six times in the 32-year record. These events may be linked to coastal filaments injecting nutrient- and phytoplankton-rich coastal waters off Oregon and northern California into the California Current. Zooplankton biomass would be expected to increase in response to the high food supply. When the source of this coastal water is cut off by detachment of the filaments from the coast (perhaps in the form of cold-core rings) the zooplankton populations decrease relatively rapidly over a period of a few months because of rapid use of the unreplenished nutrient content. This interpretation is supported by an example presented in the previous section, showing the relation between an episodic zooplankton event and satellite-inferred chlorophyll concentrations during the late winter and early spring of 1980.

ACKNOWLEDGMENTS

We are indebted to Paul Smith for graciously supplying us with the CalCOFI zooplankton data used in this study and for helpful comments on an early version of the manuscript. We also thank Larry Eber for providing us with the CalCOFI hydrographic data and John McGowan, Mark Abbott, and Tim Cowles for all of their constructive comments on the manuscript. Special thanks go to Charlie Miller for first suggesting the possibility of advection of biogeographical boundaries in the California Current and for his careful reading of the manuscript. This research was supported by NASA Grant NAGW-869 and NSF Grant OCE-831521.

LITERATURE CITED

Abbott, M.R., and P.M. Zion. 1987. Spatial and temporal variability of phytoplankton pigment off northern California during Coastal Ocean Dynamics Experiment I. J. Geophys. Res. 92(C2):1745–1756.

Allen, J.S. 1973. Upwelling and coastal jets in a continuously stratified ocean. J. Phys. Oceanogr. 3:245–257.

Alvariño, A. 1965. Distributional atlas of Chaetognatha in the California Current region. Calif. Coop. Oceanic Fish. Invest. Atlas 3.

Anonymous. 1963. CalCOFI atlas of 10-meter temperatures and salinities 1949 through 1959. Calif. Coop. Oceanic Fish. Invest. Atlas 1.

Atkinson, L.P., K.H. Brink, R.E. Davis, B.H. Jones, T. Paluszkiewicz, and D.W. Stewart. 1986. Mesoscale hydrographic variability in the vicinity of points Conception and Arguello during April–May, 1983: the OPUS 1983 Experiment. J. Geophys. Res. 91(C11): 12,899–12, 918.

Barber, R.T., and R.L. Smith. 1981. Coastal upwelling systems. *In* A.R. Longhurst (ed.), Analysis of marine ecosystems. Academic Press, London, p. 31–68.

Bernal, P.A. 1979. Large-scale biological events in the California Current. Calif. Coop. Oceanic Fish. Invest. Rep. 20:89–101.

———. 1981. A review of the low-frequency response of the pelagic ecosystem in the California Current. Calif. Coop. Oceanic Fish. Invest. Rep. 22:49–62.

Bernal, P.A., and J.A. McGowan. 1981. Advection and upwelling in the California Current. *In* F.A. Richards (ed.), Coastal upwelling. American Geophysical Union, Washington, D.C., p. 381–399.

Berner, L.D. 1967. Distributional atlas of Thaliacea in the California Current region. Calif. Coop. Oceanic Fish. Invest. Atlas 8.

Bowman, T.E., and M.W. Johnson. 1973. Distributional atlas of Calanoid copepods in the California Current region, 1949 and 1950. Calif. Coop. Oceanic Fish. Invest. Atlas 19.

Brinton, E. 1962. The distribution of Pacific euphausiids. Bull. Scripps Inst. Oceanogr., Univ. Calif. 8(2):51–270.

———. 1967. Distributional atlas of Euphausiacea (Crustacea) in the California Current region. Calif. Coop. Oceanic Fish. Invest. Atlas 5.

———. 1973. Distributional atlas of Euphausiacea (Crustacea) in the California Current region. Calif. Coop. Oceanic Fish. Invest. Atlas 18.

Chatfield, C. 1975. The analysis of time series: an introduction. Chapman and Hall, London and New York.

Chelton, D.B. 1981. Interannual variability of the California Current—physical factors. Calif. Coop. Oceanic Fish. Invest. Rep. 22:130–148.

———. 1982a. Large-scale response of the California Current to forcing by wind stress curl. Calif. Coop. Oceanic Fish. Invest. Rep. 23:130–148.

———. 1982b. Statistical reliability and the seasonal cycle: comments on "Bottom pressure measurements across the Antarctic Circumpolar Current and their relation to the wind." Deep Sea Res. v.29.

———. 1984. Seasonal variability of alongshore geostrophic velocity off Central California. J. Geophys. Res. 89(C3):3473–3486.

Chelton, D.B., and R.E. Davis. 1982. Monthly mean sea-level variability along the west coast of North America. J. Phys. Oceanogr. 12:757–784.

Chelton, D.B., P.A. Bernal, and J.A. McGowan. 1982. Large-scale interannual physical and biological interaction in the California Current. J. Mar. Res. 40(4):1095–1125.

Chelton, D.B., R.L. Bernstein, A. Bratkovich, and P.M. Kosro. 1987. The Central California Coastal Circulation Study. EOS 68(1):12–13.

Colebrook, J.M. 1977. Annual fluctuations in biomass of taxonomic groups of zooplankton in the California Current, 1955–59. Fish. Bull. 75(2):357–368.

Cutchin, D.L., and R.L. Smith. 1973. Continental shelf waves: low-frequency variations in sea level and currents over the Oregon continental shelf. J. Phys. Oceanogr. 3(1):73–82.

Davis, R.E. 1976. Predictability of sea surface temperature and sea level pressure anomalies over the North Pacific Ocean. J. Phys. Oceanogr. 6:249–266.

Denbo, D.W., and J.S. Allen. 1987. Large-scale response of atmospheric forcing of shelf currents and coastal sea level off the west coast of North America: May–July 1981–1982. J. Geophys. Res. 92(c2):1757–1782.

Enfield, D.B., and J.S. Allen. 1980. On the structure and dynamics of monthly mean sea level anomalies along the Pacific coast of North and South America. J. Phys. Oceanogr. 10:557–578.

———. 1983. The generation and propagation of sea level variability along the Pacific coast of Mexico. J. Phys. Oceanogr. 13:1012–1033.

Fleminger, A. 1964. Distributional atlas of Calanoid copepods in the California Current region, part I. Calif. Coop. Oceanic Fish. Invest. Atlas 2.

Haury, L.R. 1984. An offshore eddy in the California Current system Part IV: plankton distributions. Prog. Oceanogr. 13:95–111.

Haury, L.R., J.J. Simpson, J. Pelaez, C.J. Koblinsky, and D. Weisenhahn. 1986. Biological consequences of a recurrent eddy off Point Conception, California. J. Geophys. Res. 91(C11):12,937–12,956.

Hemingway, G.T. 1979. A description of the California Current ecosystem by factor analysis. Calif. Coop. Oceanic Fish. Invest. Rep. 20:164–177.

Hickey, B. 1979. The California Current—hypotheses and facts. Prog. Oceanogr. 8:191–279.

Kosro, P.M. 1987. Structure of the coastal current field off northern California during the Coastal Ocean Dynamics Experiment. J. Geophys. Res. 92(C2):1637–1654.

Kosro, P.M., and A.J. Huyer. 1986. CTD and velocity surveys of seaward jets off northern California, July, 1981 and 1982. J. Geophys. Res. 91(C2):7680–7690.

Kramer, D., M.J. Kalin, E.G. Stevens, J.R. Thrailkill, and J.R. Zweifel. 1972. Collection and processing data on fish eggs and larvae in the California Current region. U.S. Dept. Comm., NOAA Tech. Rep., NMFS Circ. 370, iii–iv, 1–38.

Loeb, V.J., P.E. Smith, and H.G. Moser. 1983. Ichthyoplankton and zooplankton abundance patterns in the California Current area, 1975. Calif. Coop. Oceanic Fish. Invest. Rep. 24:109–131.

McGowan, J.A., and C.B. Miller. 1980. Larval fish and zooplankton community structure. Calif. Coop. Oceanic Fish. Invest. Rep. 21:29–36.

Mooers, C.N.K., and A.R. Robinson. 1984. Turbulent jets and eddies in the California Current and inferred cross-shore transports. Science 223:51.

Nelson, C.S. 1977. Wind stress and wind stress curl over the California Current. NOAA Tech. Rep. NMFS-SSRF-714, August.

NORPAC Committee. 1960. Oceanic observations of the Pacific, 1955. The NORPAC atlas. University of California Press and the University of Tokyo Press, Berkeley and Tokyo, 123 pl. 1960.

Pedlosky, J. 1979. Geophysical fluid dynamics. Springer-Verlag, New York.

Pelaez, J., and J.A. McGowan. 1986. Phytoplankton pigment pattern in the California Current as determined by satellite. Limnol. Oceanogr. 31(5):927–950.

Raymont, J.E.G. 1980. Plankton and productivity in the oceans, volume 1, phytoplankton.

Reid, J.L. 1962. On circulation, phosphate-phosphorous content, and zooplankton volumes in the upper part of the Pacific Ocean. Limnol. Oceanogr. 7:287–306.

Simpson, J.J. 1984. An offshore eddy in the California Current system, Part III: chemical structure. Prog. Oceanogr. 13:71–93.

Smith, P.E. 1971. Distributional atlas of zooplankton volume in the California Current region, 1951 through 1966. Calif. Coop. Oceanic Fish. Invest. Atlas 13.

Smith, P.E., and R.W. Eppley. 1982. Primary production and the anchovy population in the Southern California Bight: comparison of time series. Limnol. Oceanogr. 27:1–17.

Smith, S.L., B.H. Jones, L.P. Atkinson, and K.H. Brink. 1986. Zooplankton in the upwelling fronts off Point Conception, California. *In* J.C.J. Nichoul (ed.), Marine interfaces ecohydrodynamics. Elsevier Oceanography Series 42, p. 195–213.

Traganza, E.D., J.L. Conrad, and L.C. Breaker. 1981. Satellite observations of a cyclonic upwelling system and giant plume in the California Current. *In* F.A. Richards (ed.), Coastal upwelling. American Geophysical Union, Washington, D.C., p. 228–241.

Walsh, J.J. 1977. A biological sketchbook for an eastern boundary current. *In* E.D. Goldberg, I.N. McCane, J.J. O'Brien, and J.H. Steele (eds.), The sea, volume 6, marine modeling. Wiley, New York, p. 923–968.

Wooster, W.S., and J.L. Reid. 1963. Eastern boundary currents. *In* M.N. Richards (ed.), The sea. Interscience Pub., New York, p. 253–280.

Wroblewski, J.S. 1982. Interaction of currents and vertical migration in maintaining *Calanus marshallae* in the Oregon upwelling zone—a simulation. Deep Sea Res. 29(6):665–686.

Wyllie, J.G. 1966. Geostrophic flow of the California Current at the surface and at 200 m. Calif. Coop. Oceanic Fish. Invest. Atlas 4.

Wyllie, J.G., and R.J. Lynn. 1971. Distribution of temperature and salinity at 10 meter, 1960–1969 and mean temperature, salinity, and oxygen at 150 m, 1950–1968 in the California Current. Calif. Coop. Oceanic Fish. Invest. Atlas 15.

Yoshida, K. 1967. Circulation in the eastern tropical oceans with special reference to upwelling and undercurrents. Jap. J. Geophys. 4:1–75.

APPENDIX 1
The Effects of Spurious Data on Empirical Orthogonal Functions

A perhaps surprising result from the analyses presented in this paper is the significant differences between the dominant recurring patterns of zooplankton variability with and without a $\log_e$ transformation. The first EOFs of zooplankton (Figure 16b) and $\log_e$ zooplankton (Figure 8b) are very different, and in fact suggest that very different processes control zooplankton variability. One of the motivations for using the $\log_e$ transformation in analyzing biological data is to normalize frequency distributions of observed concentrations of biological variables (Figure A1) in order to place statistical confidence limits error bars on correlations with other variables. Another common motivation is to reduce the effects of spurious outlyer data points, often attributed to sampling errors caused by patchiness in the biological variable. Although very effective as a noise filter, the transformation may also act as an effective screen for a true signal consisting of occasional pulses with anomalously large values. In this appendix, we present the results of some simulations intended to determine whether the differences between the EOFs of zooplankton and $\log_e$ zooplankton could be due to spurious observations of zooplankton volume (i.e., noise in the measurements).

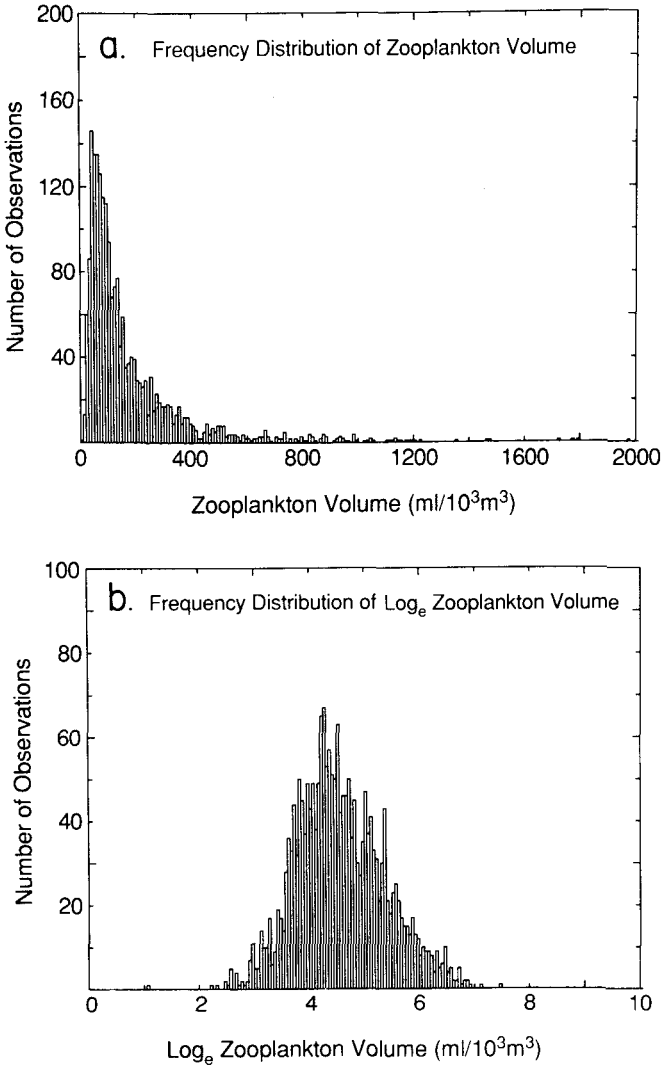

Figure A1. Frequency distributions of all samples of zooplankton displacement volumes (ml/10^3m^3) taken over the 32-year record in all 14 regions. Untransformed values (*a*) have a non-normal distribution; the $\log_e$ transformed values (*b*) have a normal distribution. The significance of untransformed values greater than 500 ml/10^3m^3 is reduced from representing 28% of the total collected zooplankton volume in the 32-year record to just over 4% of the total collected volume.

The nature of EOF analysis is to extract modes of variability that are coherent in space and time, and effectively filter out extraneous noise from each signal. If a single data set is composed of two distinct and uncorrelated signals, the analysis separates these signals into two separate modes of variability. For this reason, the addition of random uncorrelated noise to a data set does not change the spatial structure of the dominant modes extracted by the EOF analysis. It only increases the total variance of the system (and, in particular, increases the variance that is unexplained by the modes of physical or biological variability), and thus reduces the percentage of the total variance explained by the dominant modes. This capability of EOFs to extract signal from noise is shown by an example below.

The dominant EOF of the $\log_e$ transformed, seasonally corrected time series of zooplankton displacement volumes discussed in the text and shown in Figure 8b is reproduced here in Figure A2a. Spikes in zooplankton volume were randomly added to the 14 regional time series, with amplitudes ranging from two to six standard deviations from the norm. The corresponding EOF spatial patterns for these increasing noise amplitudes are shown in Figure A2b–d. The dominant EOF remains essentially unchanged, regardless of the magnitude of the added noise. EOF analysis thus very effectively extracts the underlying large-scale signal from noisy data. Figure A3 shows the percent of variance explained by the first EOF mode

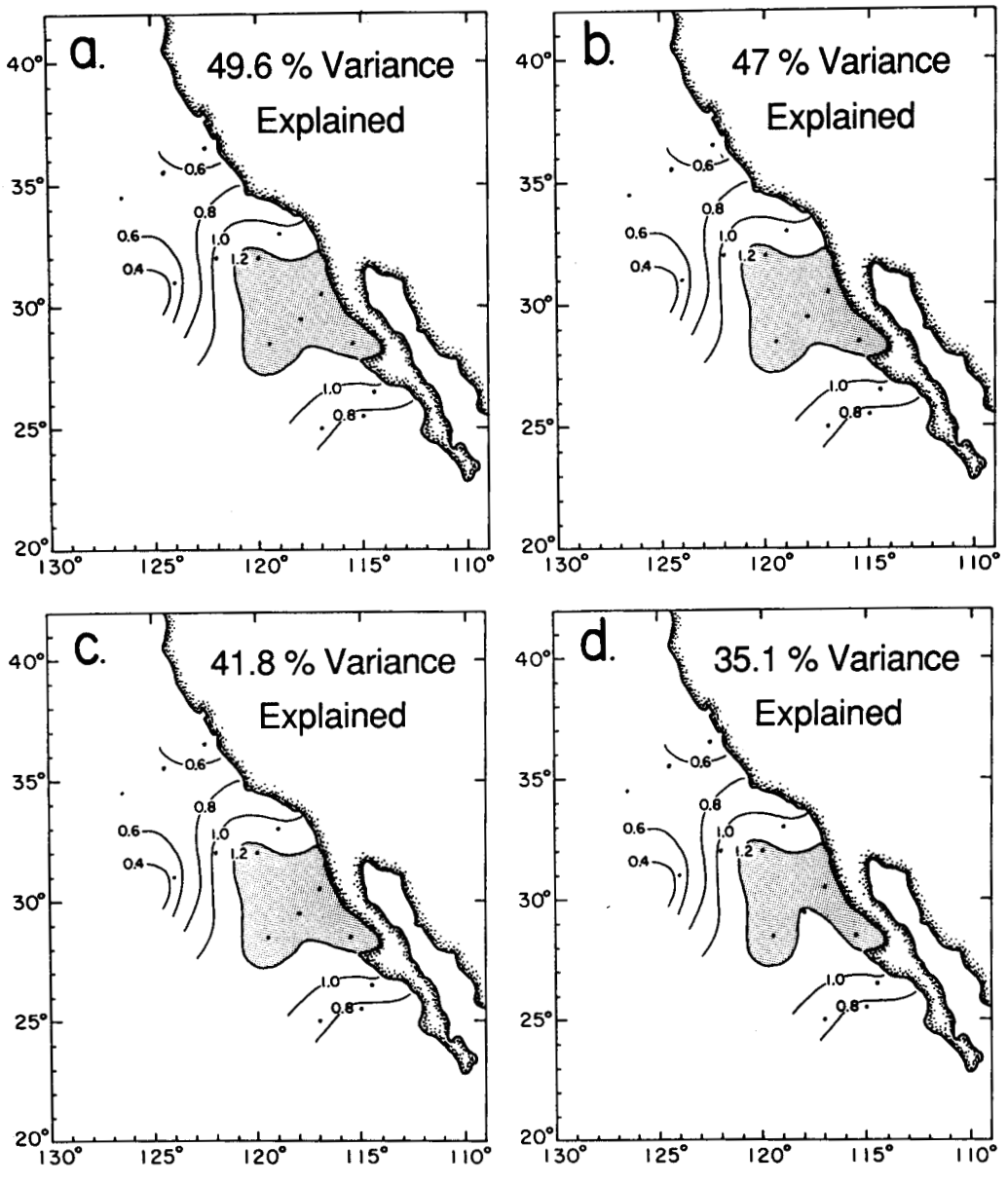

Figure A2. *a*, The dominant EOF of $\log_e$ zooplankton volume over the 14 regions denoted by dots (same as Figure 8b). The 14 time series were randomly spiked with artificial noise with amplitudes of two, four, and six standard deviations from the norm. The EOFs were recomputed from the spiked time series and are shown in *b*, *c*, and *d*.

versus the amplitude of the noise in the artificially spiked time series. The total variance explained by the first mode decreases with increasing noise amplitude. This is because the total variance unexplained by the underlying large-scale signal (i.e., the artificially added measurement noise) increases with increasing noise variance.

It can be concluded that the significant differences between the EOFs of $\log_e$ transformed and untransformed zooplankton volumes are not the result of spurious observations in the time series. The pulses present in the untransformed CalCOFI zooplankton data must therefore represent a biophysical signal that is spatially and temporally coherent throughout the CalCOFI region.

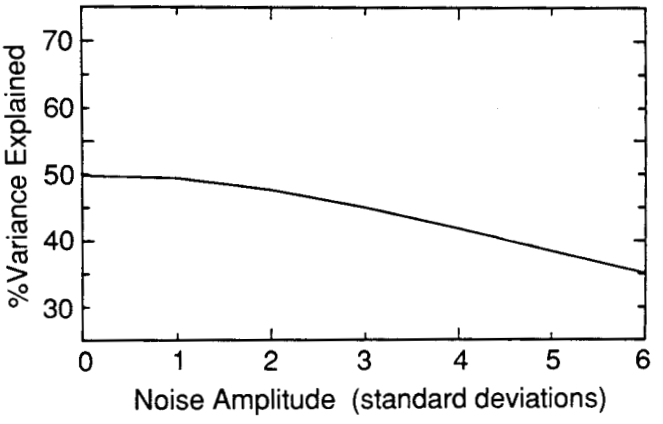

Figure A3. Percent of total variance explained by the EOFs of time series in Figure A2 versus the amplitude (in standard deviations) of the artificially added noise.

APPENDIX 2
Meridional Shifts in Zooplankton Biogeographical Boundaries in the California Current

In this appendix, distribution maps for the dominant zooplankton species in the California Current region are presented to show the interannual meridional migration of biogeographical boundaries (Figures A4–A11). These maps have been published in CalCOFI atlases 2, 3, 5, 8, 18, and 19. The dominant species in the region are broken down by taxa into four species of Chaetognatha (Alvariño 1965), four species of Thaliacea (Berner 1967), two species of Euphausiacea (Brinton 1967, 1973) and five species of Calanoid copepods (Fleminger 1964; Bowman and Johnson 1973).

During cold years (1949, 1950, 1954, and 1962) southward advection in the California Current is high, and species' biogeographical boundaries shift equatorward. During anomalously warm years (1958 and 1959) boundaries of the northern species shift northward. Southern species also shift northward, in some cases as much as 1,000 km. The implications of these shifts are discussed in detail in the text.

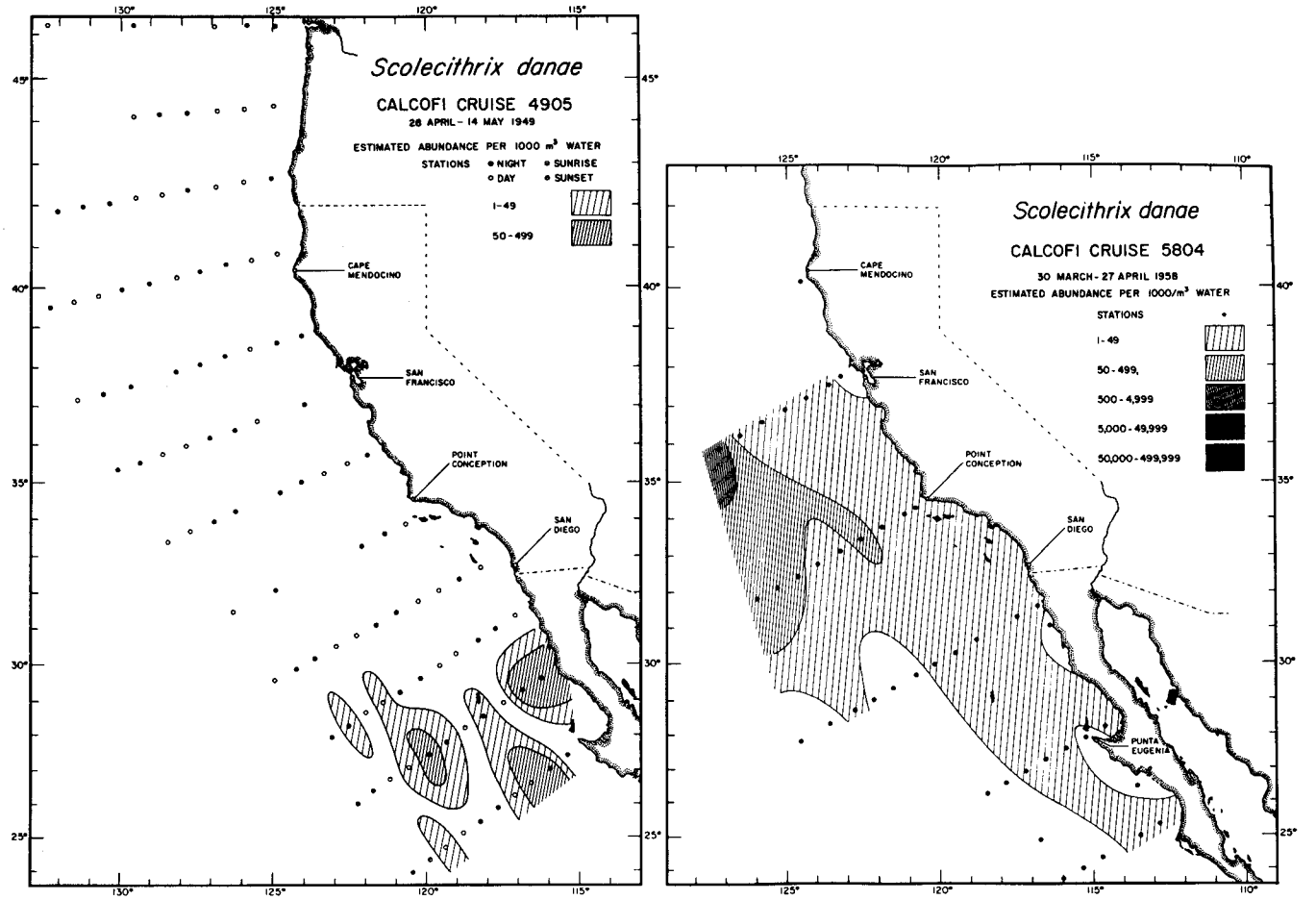

Figure A4. Distribution of *Scolecithrix danae* for May 1949 and April 1958 (Fleminger 1964; Bowman and Johnson 1973). This copepod appears to migrate northward in the low-transport year (1958).

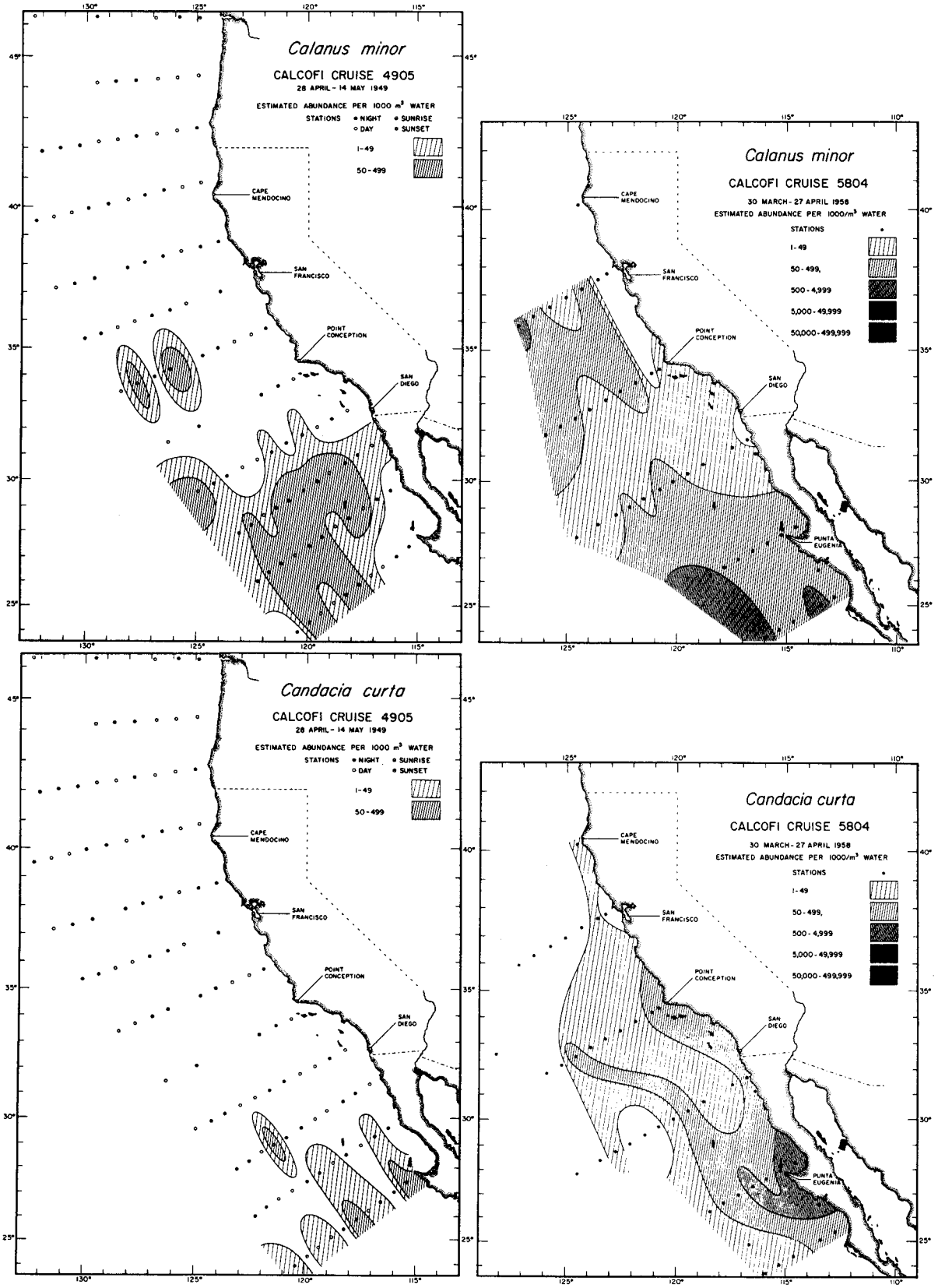

Figure A5. Distribution of *Calanus minor* and *Candacia curta* for May 1949 and April 1958 (cold and warm years, respectively; Fleminger 1964; Bowman and Johnson 1973). Note the apparent northward shifts of the biogeographical boundaries of these two southern species of copepods during the low-transport year (1958).

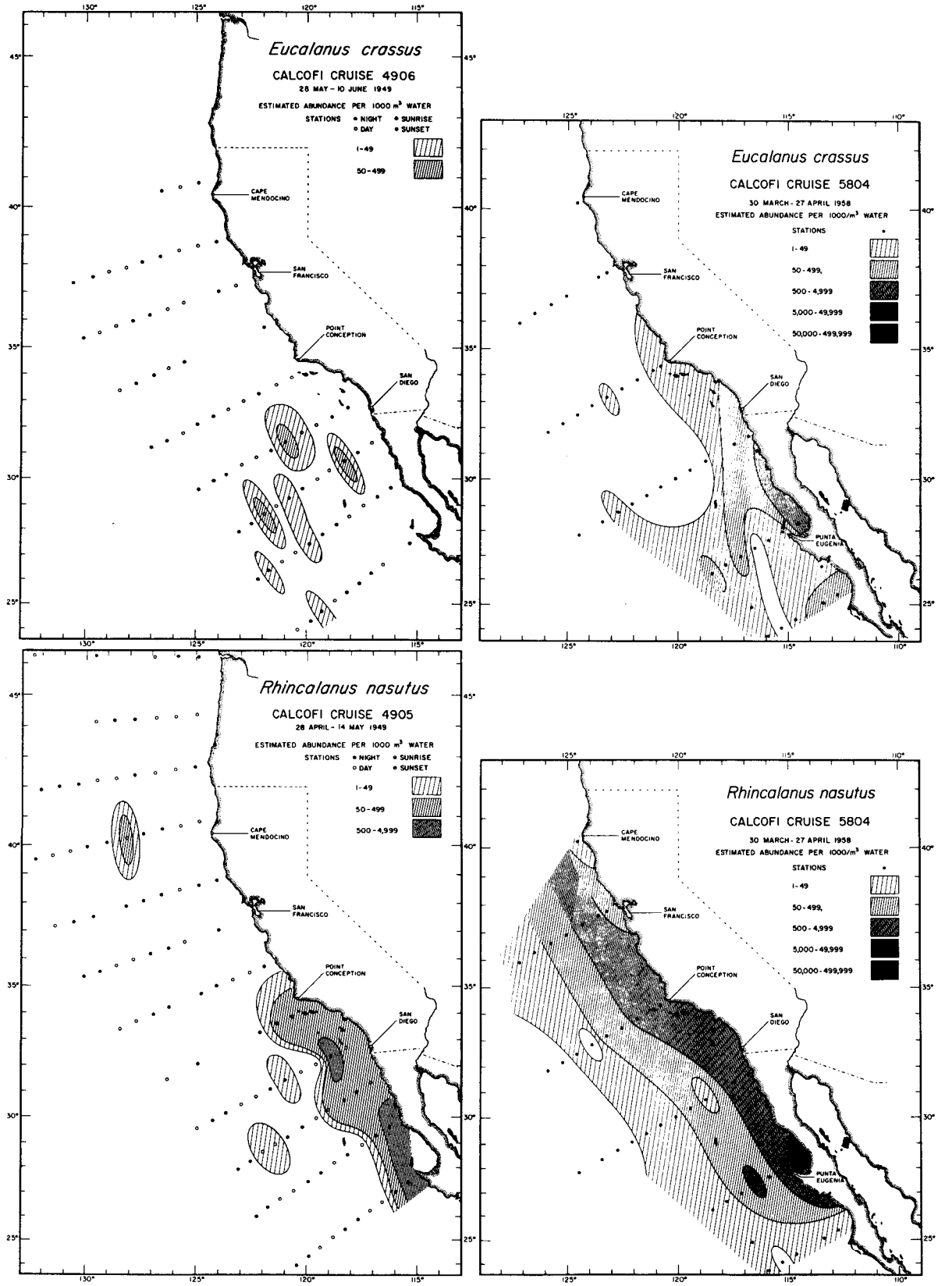

Figure A6. Distribution of *Eucalanus crassus* and *Rhincalanus nasutus* for June and May 1949 (respectively), and April 1958 (Fleminger 1964; Bowman and Johnson 1973). Contrary to what is indicated in the previous figure, these southern species appear to sustain local abundance increases during the low-advection year (1958).

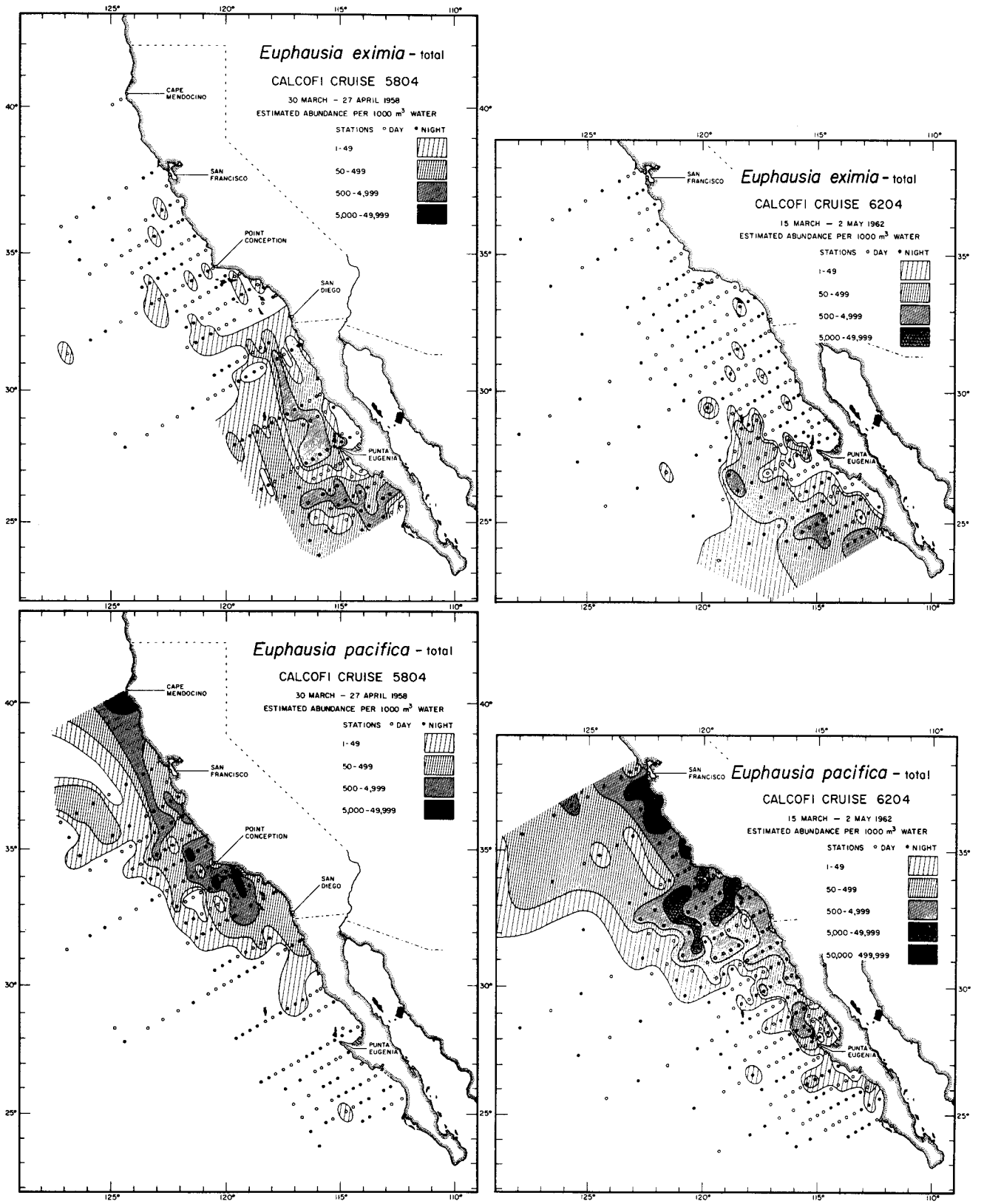

Figure A7. Distribution of *Euphausia eximia* and *Euphausia pacifica* for April of 1958 and 1962 (warm and cold years, respectively; Brinton 1967, 1973). Strong equatorward transport in 1962 pushes the species boundaries southward; weakened transport in 1958 does not bring *E. pacifica* as far equatorward, and local populations of *E. eximia* appear to increase in response to local conditions.

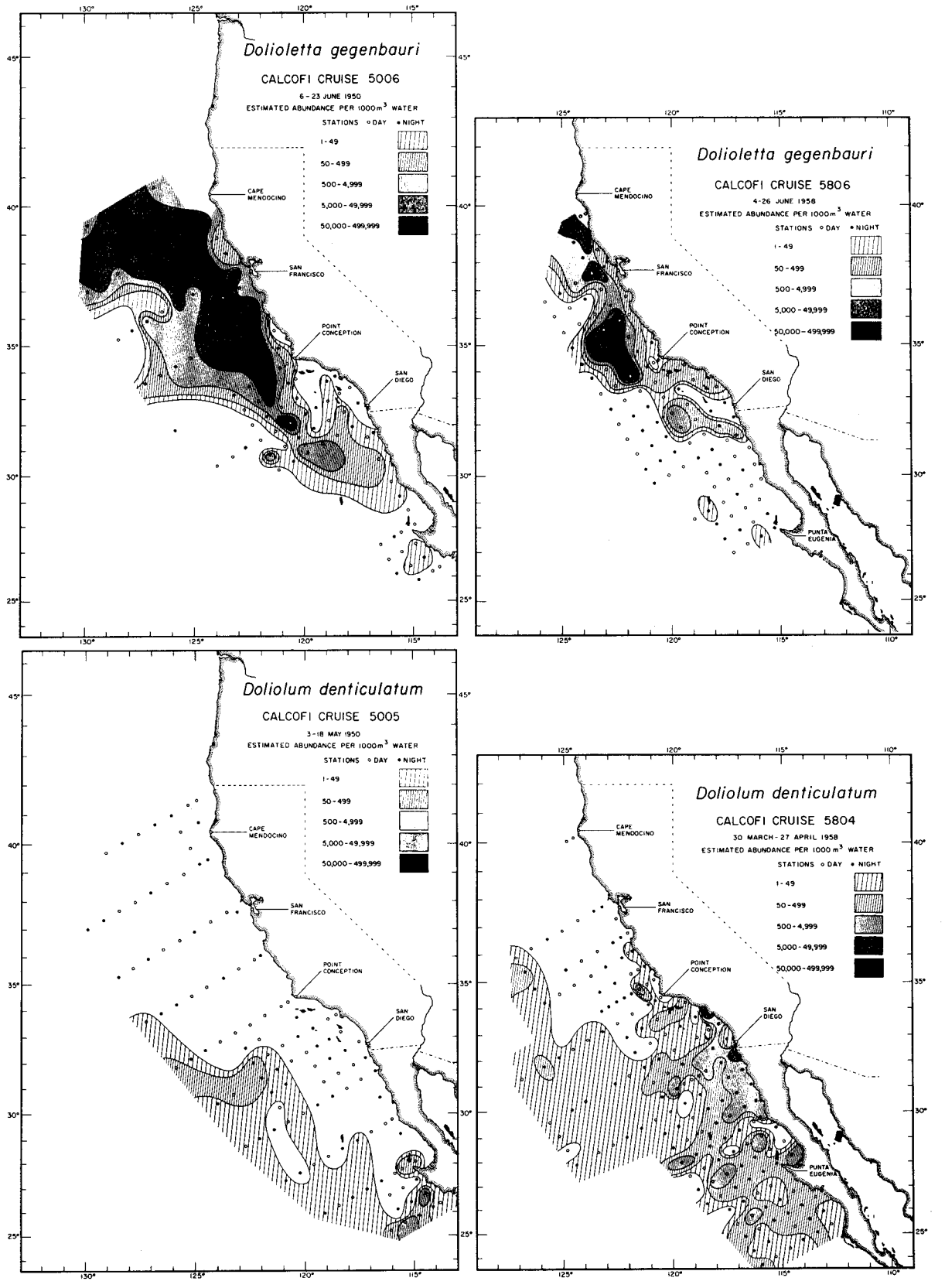

Figure A8. Distribution of *Dolioletta gegenbauri* for June 1950 and 1958, and distribution of *Doliolum denticulatum* for May 1950 and April 1958 (cold and warm years, respectively; Berner 1967). These species exhibit similar responses to advection as those in Figure A7.

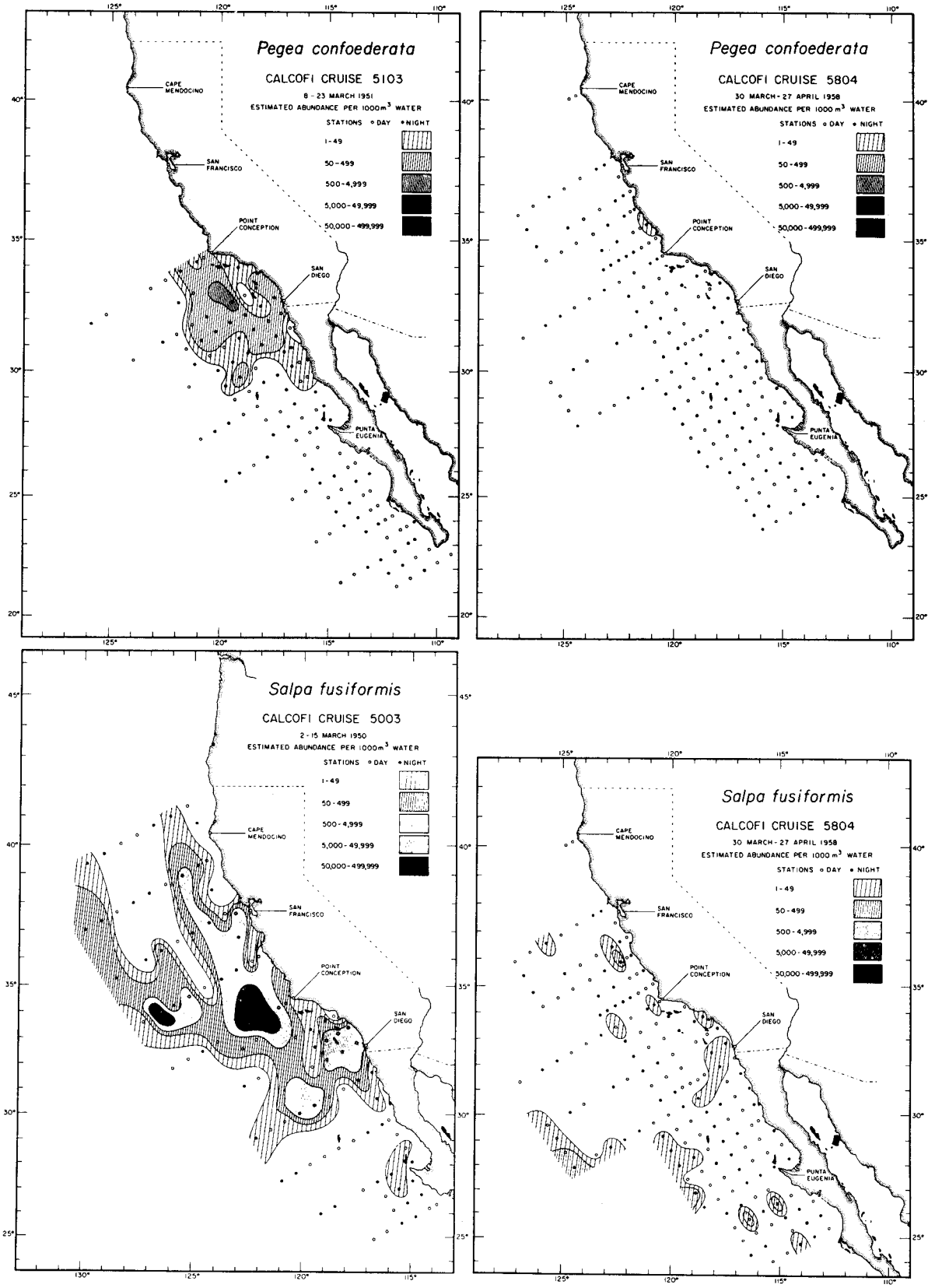

Figure A9. Distribution of *Pegea confoederata* for March 1951 and *Salpa fusiformis* for March 1950 (both cold years) and April 1958 (a warm year; Berner 1967). *P. confoederata* is present in the survey area only during the high-transport year. *S. fusiformis* undergoes a large reduction in abundance when equatorward transport decreases, leaving isolated populations in the survey area.

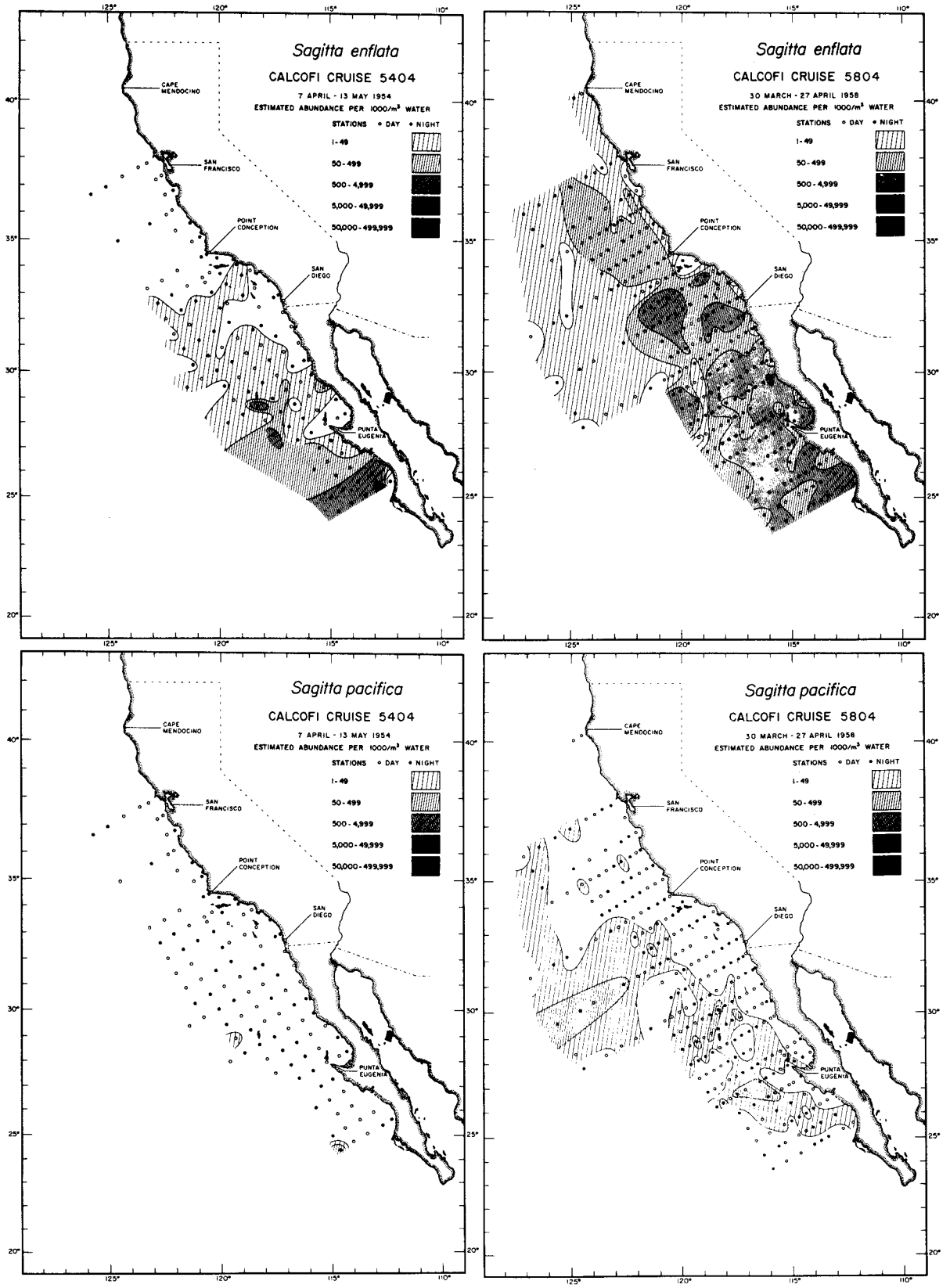

Figure A10. Distributions of *Sagitta enflata* and *Sagitta pacifica* for April of 1954 and 1958 (cold and warm years, respectively; Alvariño 1965). The biogeographical boundary of *S. enflata* appears to migrate northward during the low-transport year, compared to *S. pacifica*, which appears to move inshore, locally increasing population abundances.

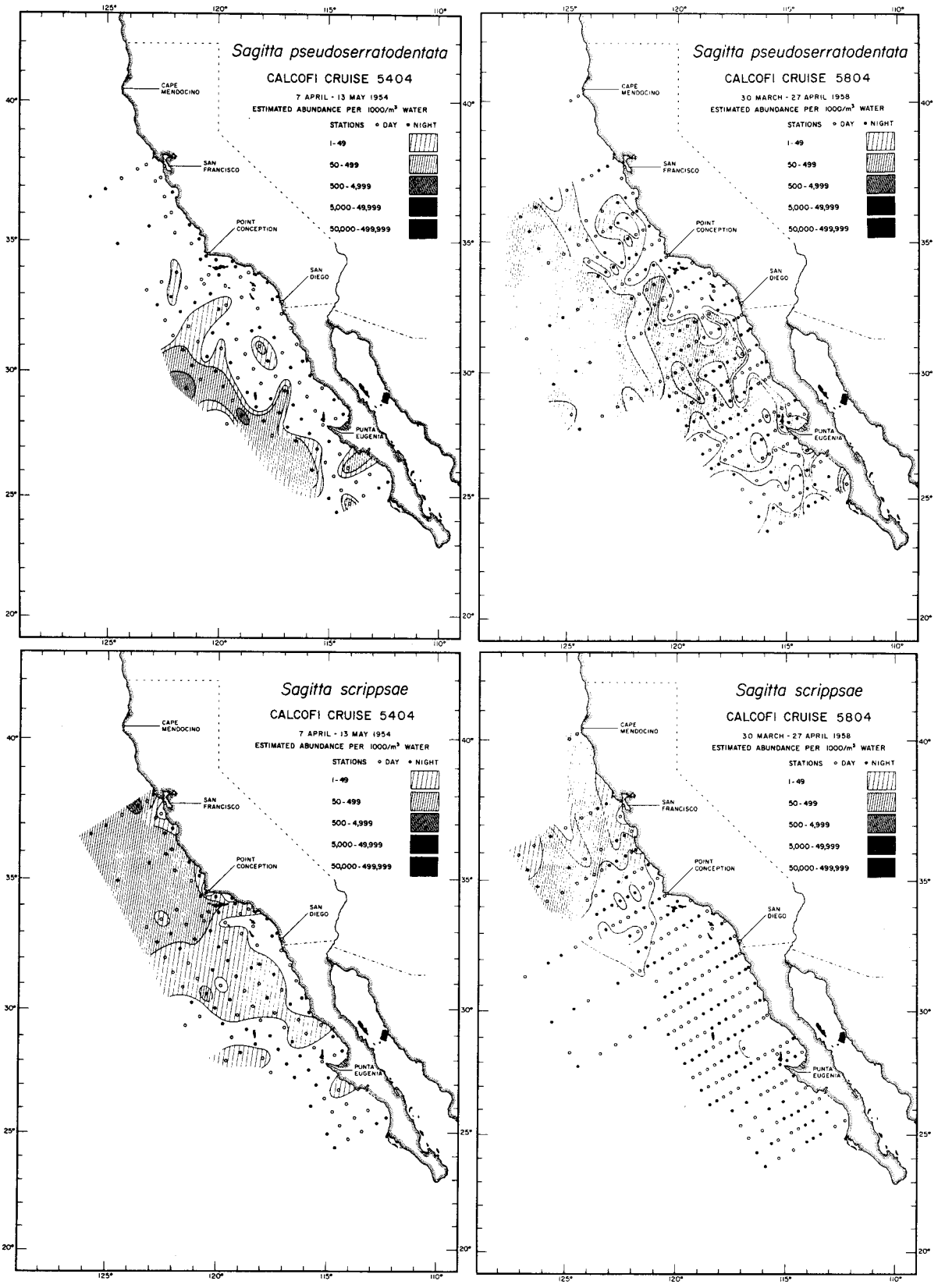

Figure A11. Distribution of *Sagitta pseudoserratodentata* and *Sagitta scrippsae* for April of 1954 and 1958 (Alvariño 1965). *S. pseudoserratodentata* locally increases abundances during the low-transport year (1958). *S. scrippsae*, a northern species, is not transported as far equatorward in the low-transport year.